The Pennsylvania State University

The Graduate School

Eberly College of Science

BIOCHEMICAL CHARACTERIZATION OF DENGUE NON-STRUCTURAL PROTEIN 5 (NS5) AND GENERAL ACID DERIVATIVES

A Thesis in

Molecular Medicine

by

Alex J. Lugo

Submitted in Partial Fulfillment
of the Requirements
for the Degree of

Master of Science

August 2011

The thesis of Alex J. Lugo was reviewed and approved* by the following:

Craig E. Cameron
Paul Berg Professor of Biochemistry and Molecular Biology
Thesis Adviser

Tracy Nixon
Professor of Biochemistry and Molecular Biology

Leslie J. Parent
Associate Professor of Medicine, and Microbiology and Immunology

Anthony Schmitt
Associate Professor of Molecular Immunology and Infectious Diseases

Adam Glick
Associate Professor, Department of Veterinary and Biomedical Sciences
Head of the Department of Molecular Medicine

*Signatures are on file in the Graduate School.

Abstract

Dengue virus (DV) is a current global health problem affecting tropical and sub-tropical regions. The existence of four dengue serotypes renders individuals who are partially protected against one serotype to be even more vulnerable to severe disease caused by another. Therefore, development of a vaccine will require a broad mechanism for virus attenuation. Dengue virus non-structural protein 5 (DV NS5) is the viral RNA-dependent RNA polymerase (RdRp). The poliovirus system has suggested that the fidelity of a viral RdRp can be targeted for viral attenuation and vaccine development. Most studies of Dengue non-structural protein 5 (DV NS5) have focused on *cis*-acting elements or qualitative determinants of polymerase function. The goal of this study was to acquire the first quantitative perspective of DV NS5 structure-function relationships. The major findings were: (1) The methyltransferase domain of DV NS5 is required for optimal RdRp activity; (2) DV NS5 has a preference for triphosphorylated primers; (3) A conserved motif-D lysine is required for nucleotidyl transfer efficiency in DV NS5. In addition, an assay to characterize the kinetics of nucleotide binding and elongation has been developed.

Table of Contents

List of Tables

List of Figures

Acknowledgments

First, I would like to thank Dr. Craig E. Cameron for all his support, advice and the opportunity to work in this research. I would like to thank the members of the Cameron laboratory, especially Dr. Jamie Arnold who helped me in the early stages of my project and Eric Smidansky for his invaluable insight on enzyme kinetics.

Finally, I would like to thank those closest to me, for their love and support throughout this graduate work experience. I thank my mom, Ana and my father, Jorge for their support and encouragement. Finally but not least, I thank my wife, Yesenia and my son, Alex for embarking in this journey with me and for being part of my life.

Chapter 1

Introduction

Viruses of the *Flaviviridae* Family are Important Human Pathogens

Two important human pathogens that belong to the *Flaviviridae* family are dengue virus (DV) and hepatitis C virus (HCV). Damage from HCV infection is the major cause of liver transplants in the United States, and the virus is distributed worldwide. The main route of transmission is through contact with infected body fluids. HCV is the only member of the *Hepacivirus* genus, and has 6 genotypes that differ by 30 to 35% at the RNA genome nucleotide level. The HCV genome is a 9.6 kb positive-strand RNA that encodes three structural proteins and seven non-structural (NS) proteins (Fig. 1A). Non-structural protein 5B (NS5B) encodes the RNA dependent RNA polymerase (RdRp) (Fig. 2A,B). The standard therapy has been a combination of ribavirin and interferon-α, which was effective in only 50% of patients [1-4]. A protease inhibitor against NS3, recently approved by the FDA, is now used in a combination with ribavirin and interferon-α to treat non-responders [5].

Dengue virus belongs to the *Flavivirus* genus. It is an arthropod-borne disease of global importance. The vector that transmits and spreads the virus is the mosquito *Aedes aegypti*. The mosquito vector is endemic to tropical and sub-tropical regions, and global warming has raised health concerns because of expansion of the range in which the insect reproduces [6]. Disease caused by

dengue virus is characterized by fever, headache, nausea, and vomiting and can develop into dengue hemorrhagic fever (DHF), leading to vascular leaking and possible death. The risk is heightened when a person has developed immunity against one serotype, and later in life is infected by a different serotype. This occurs because pre-existing antibodies recognize the new serotype of the infecting virus, and partially neutralized antibody-virus complexes are taken up by macrophages. Once inside the macrophages, the virus replicates, and the secretion of vasoactive mediators by these cells may lead to an increase in vascular permeability causing hemorrhage. This is known as antibody-dependent enhancement (ADE) [7, 8]. The only treatment available is palliative.

Dengue virus has a 10.8 kb positive-strand RNA genome that encodes three structural proteins and seven non-structural proteins (Fig. 1B). Non-structural protein 5 (NS5) exhibits two activities. A methyltransferase domain is involved in capping of the viral RNA for translation, and the RNA-dependent RNA polymerase domain replicates the genome (Fig. 2C,D) [9-11].

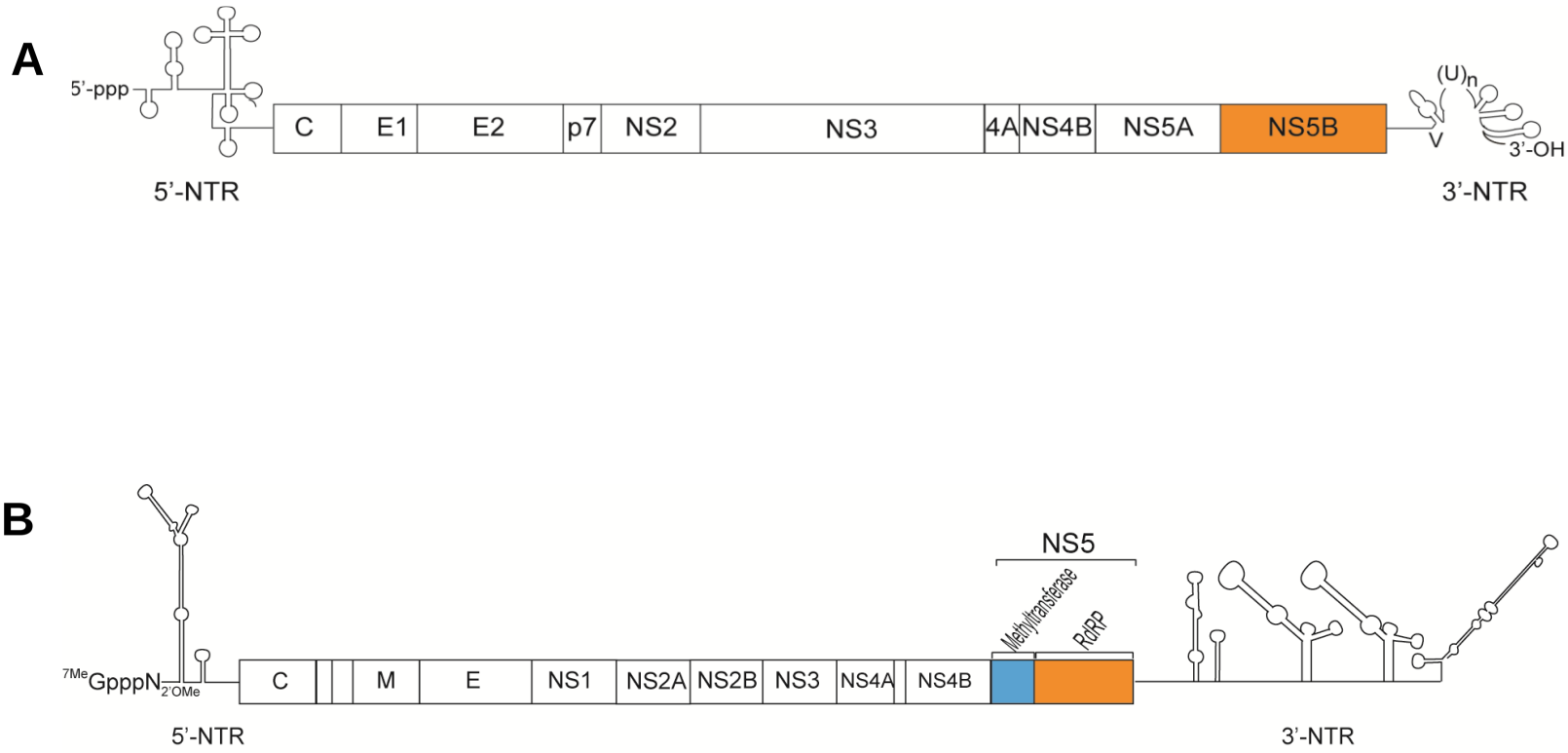

Figure 1: HCV and Dengue Virus Genomes. Both viruses have a positive-strand RNA genome of approximately 10 kb. Each encodes a single polyprotein that is cleaved into three structural proteins and seven non-structural proteins. **(A)** HCV genome. The NS5B gene encodes the RdRp domain. **(B)** DV genome. The NS5 encodes both the methyltransferase domain and the RdRp domain.

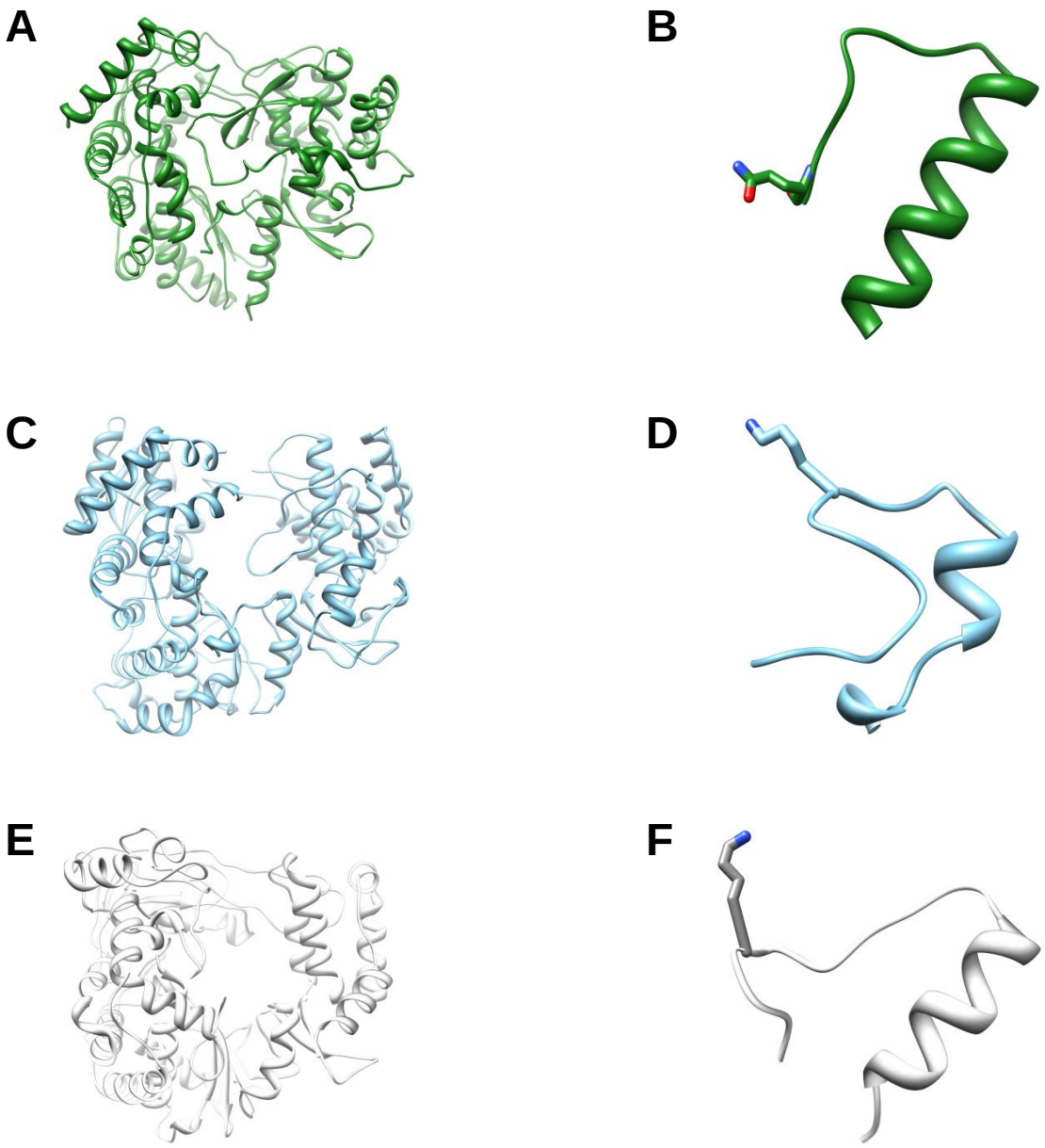

Figure 2: Crystal Structures of HCV NS5B, DV RdRp and PV RdRp. DV RdRp and HCV NS5B have a priming loop occluding the active site, a structural feature characteristic of enzymes that initiate *de novo.* **(A)** HCV NS5B structure (PDB: 1C2P). **(B)** HCV NS5B motif-D showing the position of the glutamine residue. **(C)** DV RdRp structure (PDB: 2J7U). **(D)** Dengue RdRp motif-D showing the position of the lysine general acid residue. **(E)** PV RdRp structure (PDB: 1RA6). PV RdRp has an open active site allowing the enzyme to stably utilize double-stranded RNA substrate *in vitro*. **(F)** PV RdRp motif-D showing the position of the lysine general acid residue.

Two-metal-ion Mechanism for Nucleotidyl Transfer and the Role of the General Acid

All living organisms and viruses make use of nucleic acid polymerases to replicate their genetic material. Nucleic acid polymerases employ a two-metal-ion mechanism for nucleotidyl transfer. In this mechanism, Mg^{2+} ion B enters the active site bound to the triphosphate moiety of the incoming nucleoside triphosphate substrate. Mg^{2+} ion B is coordinated by aspartate residues located in motif A and the phosphate groups of the nucleotide triphosphate. Mg^{2+} ion B orients the triphosphate moiety in the active site. A second Mg^{2+} ion is coordinated by the 3'-hydroxyl of the nascent RNA, the incoming nucleotide α-phosphate, and aspartate residues in motifs A and C. The function of metal A is to facilitate deprotonation of the 3'-hydroxyl by lowering the pKa. This sets the stage for subsequent nucleophilic attack of the α-phosphorous atom. As the transition state is reached, the 3'-hydroxyl proton is transferred to an unidentified acceptor [12-14] (Fig. 3). In addition, recent work from the Cameron laboratory demonstrated the direct involvement of an active-site amino acid residue in the nucleotidyl transfer reaction. The function of this residue is to protonate the pyrophosphate leaving group, thus accelerating the reaction [15] (Fig. 3). Castro and co-workers demonstrated in the RNA-dependent RNA polymerase from poliovirus (PV) (Fig. 2E,F), the RNA-dependent DNA polymerase from HIV Reverse transcriptase, the DNA-dependent DNA polymerase from bacteriophage RB69, and the DNA-dependent RNA polymerase from bacteriophage T7 that the function of this amino acid residue is conserved in all four classes of nucleic acid

polymerases [15]. This amino acid residue has been implicated in influencing the replication speed and error frequency in poliovirus (Cameron unpublished data).

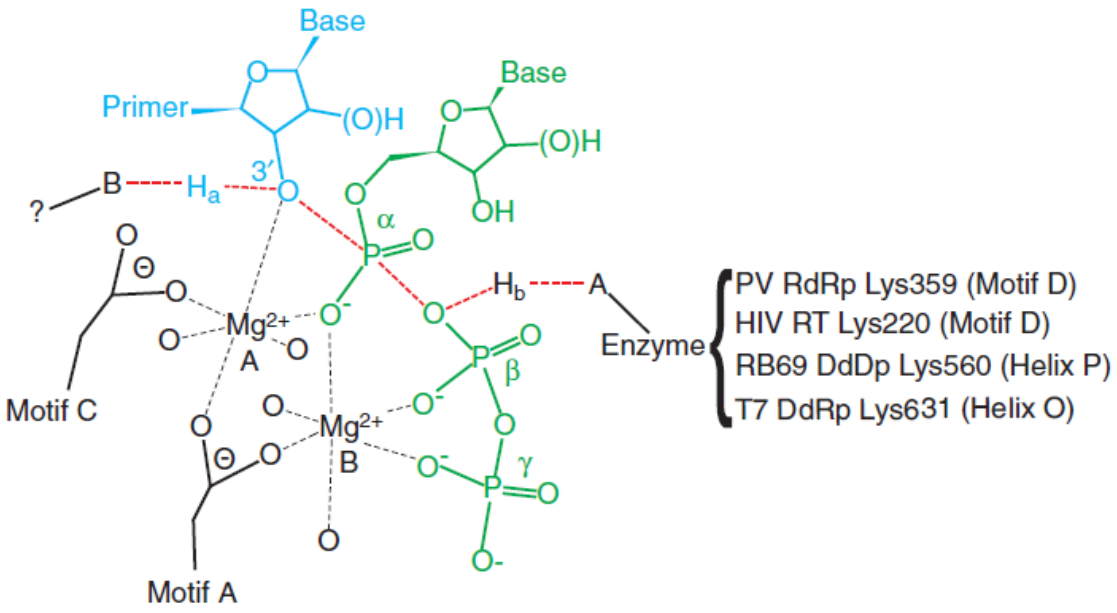

Figure 3: Two-metal-ion Mechanism for Nucleotidyl Transfer. A Mg^{2+} ion (metal B) enters with the nucleoside triphosphate (green). This divalent cation is coordinated by an aspartate residue in motif A, phosphates of the incoming nucleotide, and water molecules. The function of metal B is to orient the triphosphate in the active site. A second Mg^{2+} (metal A) is coordinated by aspartate residues in motif A and C, the 3'-hydroxyl of the primer terminus (blue), and the α-phosphate of the incoming nucleotide. The function of metal A is to lower the pKa of the 3'-hydroxyl facilitating nucleophilic attack on the α-phosphorous atom. As the transition state is reached, the primer 3'-hydroxyl proton is transferred to an unidentified acceptor (B). In addition, a proton is donated to the pyrophosphate leaving group by an amino acid residue (A) that serves as a general acid catalyst. Adapted from [15].

A Universal Strategy to Design a Vaccine

In vitro mutational studies done with the PV RdRp (Fig. 2E) suggested that changes in the amino acid residue occupying the general acid position (Fig. 2F) affect replication speed and fidelity. A change from Lys to Arg or to His decreased the nucleotide incorporation rate constant from 90 s^{-1} to 5 s^{-1}, and increased fidelity of the K359R and K359H derivatives (Table 1) (Smidansky, Maksimchuk and Cameron unpublished). Moreover, a genetically engineered poliovirus containing Arg at the general acid position of the RdRp was shown to protect mice against a challenge with a lethal dose of wild-type virus (Lee, August and Cameron unpublished). Thus, a rational approach to vaccine design might be through development of viruses with an altered RdRp general acid catalyst amino acid residue leading to defective virus replication.

	Mutation Frequency		
Allele	Sequencing	Kinetics	Nucleotide Incorporation Rate Constant
WT	2	1/6,000	$90 \pm 5\ s^{-1}$
K359H	nd	1/13,500	$5.0 \pm 0.5\ s^{-1}$
K359R	nd	1/9,000	$5.0 \pm 0.5\ s^{-1}$

Table 1: Mutation Frequency and Nucleotide Incorporation Rate Constant of PV RdRp General Acid Derivatives. A change in the general acid (position 359) from Lys to Arg or His reduced the nucleotide incorporation rate constant by approximately 20 fold. Enhanced fidelity of the polymerase was observed for K359H and K359R with respect to WT (Cameron unpublished data).

Conservation of the Putative General Acid in DV2 NS5, but not in HCV NS5B

A striking difference between the HCV RdRp and all other known nucleic acid polymerases is lack of conservation in the HCV enzyme at the general acid position, which can be occupied by Lys, Arg or Gln in different isolates (Fig. 4A). Most surprising was the presence of Gln, which lacks a dissociable proton to function as a general acid. The thought was that the nature of the amino acid residue at this position perhaps correlated with replication speed and fidelity in HCV NS5B. It was further hypothesized that failure of antiviral therapy might be linked to the nature of the residue at this position, but *in vitro* biochemical assays revealed no differences in kinetic behavior between different HCV NS5B general acid derivatives. We wondered if lack of conservation at the general acid position was a feature of *Flaviviridae* as a group. However, in DV NS5 the amino acid residue at the general acid position is well conserved across the four different serotypes, suggesting that the function of this amino acid might also be conserved (Fig. 4B).

A

HCV subtype 1b (isolate Con1)	351	GDPP	K PEYDL
HCV subtype 2a (isolate JFH-1)	351	GDPP	R PEYDL
HCV subtype 1a (ACJ37207.1)	351	GDPP	Q PEYDL
HCV subtype 1a (ACJ37201)	351	GDPP	Q PEYDL
HCV subtype 1b (AAK08509)	351	GDPP	Q PEYDL
HCV subtype 1b (ACE82441)	351	GDPP	Q PEYDL
HCV (isolate BK)	351	GDPP	Q PEYDL

B

DENV-1/BR/BID-V2395/2006	684	MGKVR	K DIPQW
DENV-1/BR/BID-V3490/2008	684	MGKVR	K DIPQW
DENV-2/MX/BID-V3356/1992	684	MGKVR	K DIQQW
DENV-2/BR/BID-V2382/2002	684	MGKVR	K DIQQW
DENV-3/VE/BID-V2454/2001	684	MGKVR	K DIPQW
DENV-3/TH/BID-V2321/2001	684	MGKVR	K DIPQW
DENV-4/PH/BID-V3361/1956	684	MGKVR	K DIPQW
DENV-4/VE/BID-V2490/2007	684	MGKVR	K DIPQW

Figure 4: Sequence Alignments of DV NS5 and HCV NS5B in the Vicinity of the General Acid Position. (A) HCV NS5B sequence alignments ± 5 amino acids from the general acid position. Two important isolates, Con1 and JFH-1, harbor a Lys and Arg, respectively. Most isolates posses Gln at position 355. **(B)** DV NS5 sequence alignments ± 5 amino acids from the general acid position. Lys is conserved across the four different Dengue serotypes.

Viral Polymerases from the Flaviviridae Family Utilize a *De novo* Initiation Mechanism for RNA Synthesis

Two initiation mechanisms are known for viral RdRps: primer-dependent initiation and *de novo* initiation (Fig. 5). DV NS5 and HCV NS5B use the latter mechanism for initiation. Three steps have been proposed for RNA synthesis by polymerases that initiate *de novo*: initiation, initiation to elongation transition, and elongation [16]. Structural evidence from the bovine viral diarrhea virus (BVDV) polymerase in complex with GTP indicates the existence of a GTP binding site in the polymerase, known as the *i* site. During *de novo* initiation, GTP binds to the *i* site serving as primer by providing the 3'-OH for the formation of the first phosphodiester bond [17].

In vitro, DV NS5 and HCV NS5B have the ability to initiate *de novo* in the presence of high concentrations of GTP or initiate in a primer-dependent manner utilizing short primers for the elongation of RNA [17-24]. The accumulation of short abortive products has been observed for *de novo* initiation *in vitro* [16]. Recent *in vivo* evidence demonstrates the accumulation of abortive transcripts in *E. coli* [25]. Interestingly, in our assays short primers are used more efficiently than GTP suggesting that formation of short products observed during *de novo* initiation could be a requirement for efficient elongation of viral RNAs *in vivo*.

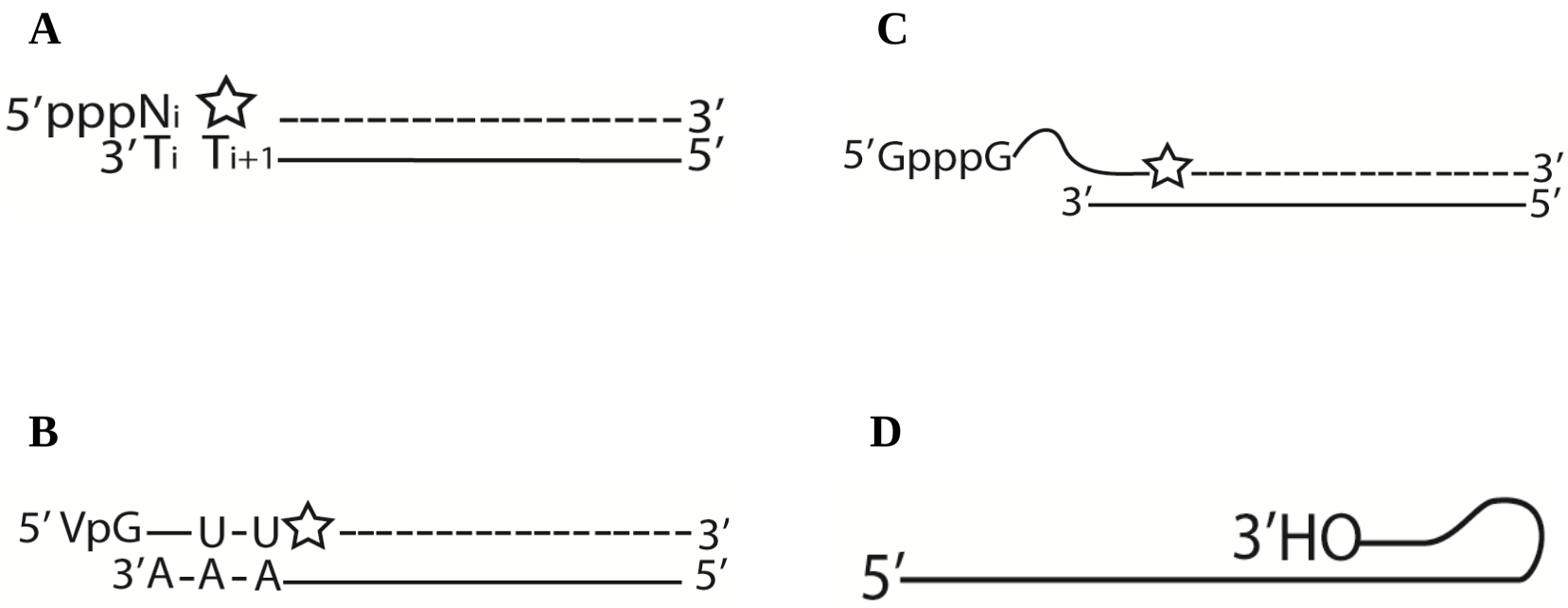

Figure 5: Schematics of Viral Initiation Mechanisms. The star represents the first nucleotide incorporated, and the dashed line the newly synthesized viral RNA. **(A)** In *de novo* initiation a nucleoside triphosphate ($pppN_i$) occupies the initiation site in the polymerase providing the 3'-OH for the formation of the phosphodiester bond. An incoming nucleotide pairs with the T_{i+1} site and a phosphodiester bond is formed. **(B)** In protein-primed initiation, a Tyr residue of poliovirus protein VPg provides the 3' OH for formation of the first phosphodiester bond to a uridylate residue (U). **(C)** In the cap-snatching initiation mechanism, influenza virus PA protein decaps cellular mRNA and removes downstream sequence between 9 to 17 nucleotides in length. This 5' cap plus RNA serves as a primer to elongate the viral RNA. **(D)** Template-primed initiation, also known as copy-back, is observed *in vitro*. The 3' end of the RNA template is used as a primer to extend the RNA. Adapted from [16]

The overall goal of this study was to develop the first quantitative perspective of DV structure-function relationships. First, we demonstrated the role of the methyltransferase domain in DV RdRp enzymatic activity. Second, we found that triphosphorylated dinucleotides are preferred for initiation by DV NS5, but the same preference was not observed for HCV NS5B, suggesting that enzymes with their own capping machinery may have higher affinity for triphosphorylated primers. Third, DV NS5 general acid derivatives showed a reduction in specific activity, confirming that use of the general acid catalyst occurs within the *Flaviviridae* family. HCV NS5B does not appear to require the general acid. Last, we are the first to describe on an assay to study the kinetics of binding and elongation for DV NS5.

Chapter 2

Materials and Methods

Cloning of pET22-HCV-NS5B-CHis

To make a construct with a 6x-His tag at the carboxyl terminus, the plasmid pET22-Sumo-HCV-NS5B was used as a PCR amplification target for the NS5B gene with primers 1 and 2 (Table 2). The pET22 vector and the PCR product were digested with XbaI/XhoI, ligated and transformed into DH5-α cells. The efficiency of transformation was determined, and colonies were grown overnight. Plasmid DNA was isolated following standard laboratory procedures and screened with XbaI/XhoI. A DNA midi-prep was performed for a positive clone, and the plasmid sent for sequencing. pET22-HCV-NS5B-K355R-CHis was made by overlap extension PCR using pET22-HCV-NS5B-CHis as the template and primers 1 and 4 (PCR 1) and primers 2 and 3 (PCR 2). PCR 1 and PCR 2 were used as templates to make the HCV NS5B K355R gene (PCR 3). The pET22-HCV-NS5B-K355Q-CHis was made using primers 1 and 6 and primers 2 and 5 as described above.

Cloning of pET26Ub-Den-NS5-CHis and pET26Ub-Den-RdRp-CHis

The plasmid pET22-Sumo-Den2-NS5 was used to amplify the DV NS5 gene using primers 1 and 2 (Table 3). The purified PCR product and the vector pET26Ub were digested with SacII and HindIII. A ligation reaction was performed and transformed into DH5-α cells. The efficiency of transformation was

determined, and colonies were grown overnight. Plasmid DNA was isolated following standard laboratory procedures and screened with SacII and HindIII. A DNA midi-prep was performed for a positive clone, and the plasmid was sent for sequencing.

The plasmids harboring Arg, His or Gln at position 689 were obtained by doing overlap extension PCR using the plasmid pET26Ub-Den2-NS5-CHis as a template. For pET26Ub-Den2-NS5-K689R-CHis, primers 3 and 5(PCR 1) and 2 and 4 (PCR 2) were used. For pET26Ub-Den2-NS5-K689H-CHis, primers 3 and 7 (PCR 1) and 6 and 8 (PCR 2) were used. For pET26Ub-Den2-NS5-K689Q-CHis, primers 3 and 10 (PCR 1) and 2 and 9 (PCR 2) were used. Overlap extension PCR was set up with PCR 1 and PCR 2 for all the plasmids, and standard laboratory protocols were used to purify and isolate the plasmid DNA. pET26Ub-Den2-RdRp-CHis was obtained using pET26Ub-Den2-NS5-CHis as the template and primers 2 and 11.

Table 2: Primers Used for HCV NS5B Constructs

Id Number	Primers	Sequence
1	HCV-Con1-NS5B-XbaI-for	5'-GCGGAATTCTCTAGAAATAATTTTGTTTAACTTTA AGAAGGAGATATACCATGAGCA TGTCCTACACA-3'
2	HCV-NS5B-GSSG-H6-XhoI-rev	5'-GCGGAATTCCTCGAGCTATTAATGGTGGTGATGG TGGTGACCAGAGGATCCCCG GGGTCGGGCACG-3'
3	H5b.Con1-K355R-For	5'-CCTGGGGACCCGCCCCGCCCAGAATACGACTTG-3'
4	H5b.Con1-K355R-Rev	5'-CAAGTCGTATTCTGGGCGGGGCGGGTCCCCAGG-3'
5	H5b.Con1-K355Q-For	5'-CCTGGGGACCCGCCCCAGCCAGAATACGACTTG-3'
6	H5b.Con1-K355Q-rev	5'-CAAGTCGTATTCTGGCTGGGGCGGGTCCCCAGG-3'

Table 3: Primers Used for DV NS5 and DV RdRp Constructs

Id Number	Primers	Sequence
1	NS5-SacII-Ub-for	5'-GCGACTAGTCCGCGGTGGAGGAACTGGCAACATAGGA-3'
2	NS5-HindIII-6xHis-rev	5'-GCGCTCGAGAAGCTTTTACTAATGGTGGTGATGGTGGTG ACCAGAGGATCCCCACAGAC-3'
3	NS5-1200-for	5'-GACCAAGACCACCCATACAAA-3'
4	NS5-K689R-for	5'-AAAGGTTAGGAGGGACATACAACAATGGGAA-3'
5	NS5-K689R-rev	5'-GTTGTATGTCCCTCCTAACCTTTCCCATGTCAT-3'
6	NS5-K689H-for	5'-ATGGGAAAGGTTAGGCATGACATACAACAATGGGAACC TTCAAGAGGA-3'
7	NS5-K689H-rev	5'-TATGTCATGCCTAACCTTTCCCATGTCATTTAG-3'
8	NS5-PstI-HindIII-rev	5'-GCGCTCGAGAAGCTTCTGCAG TTACTAATGGTGGTGATGGTGGTG-3'
9	NS5-K689Q-for	5'- AAAGGTTAGGCAGGACATACAACAATGGGAA-3'
10	NS5-K689Q-rev	5'-GTTGTATGTCCTGCCTAACCTTTCCCATGTCAT-3'
11	RdRp-SacII-Ub-forward	5'-GCGACTAGTCCGCGGTGGAAACCTAGACATAATCGG G-3'

Expression and Purification of CHis Proteins

DV NS5 and DV RdRp were expressed in Rosetta (DE3) pUbpS cells at 15 °C for 48 hours utilizing an auto-induction media. HCV NS5B was expressed in Rosetta (DE3) cells at 15 °C for 48 hours. When OD_{600} was higher than 7, cells were harvested and stored at -80 ºC. In addition, expression was confirmed by SDS-PAGE. Frozen cell pellets were thawed on ice and suspended in lysis buffer (100 mM potassium phosphate, pH 8.0, 500 mM NaCl, 5 mM 2-mercaptoethanol, 20% glycerol for HCV or 10% glycerol for DV, 1.4 µg/mL leupeptin and 1.0 µg/mL pepstatin A), with 5 mL of lysis buffer per gram of cells. The suspended cells were passed through a 50 micron nylon mesh. The filtered suspended cells were passed twice through a microfluidizer (model M-110EH-30; Microfluidics International Corporation, Newton, MA) at 15,000 psi. Phenylmethylsulfonylfluoride (PMSF) and NP-40 were added to a final concentration of 1 mM and 0.1% (v/v), respectively. While stirring the lysate, polyethylenimine (PEI) was slowly added to a final concentration of 0.25% (v/v). The lysate was stirred for an additional 30 min at 4 °C after the last addition of PEI, and then centrifuged at 24,000 rpm for 30 min at 4 °C. The PEI supernatant was decanted to a fresh beaker, and while stirring, ammonium sulfate was slowly added to 40% (w/v) saturation. This supernatant was stirred for 30 min after the last addition of ammonium sulfate, and centrifuged at 24,000 rpm for 30 min at 4 °C. The supernatant was decanted, and the pellet was suspended in equilibration buffer (100 mM potassium phosphate, pH 8.0, 500 mM NaCl, 5 mM 2-

mercaptoethanol, 20% glycerol, 1.4 µg/mL leupeptin, 1.0 µg/mL pepstatin A, 5 mM imidazole and 0.1% NP-40).

The total protein concentration was determined by Bradford assay, and a nickel-nitrilotricacetic acid (Ni-NTA) column was packed. One mL of nickel resin was used for every 10 mg of tagged protein. The amount of tagged protein was determined by an approximation, assuming 10% of the total protein was tagged protein. The Ni column was equilibrated with 10 column volumes (CV) of equilibration buffer. Once the column was equilibrated, the resin was transferred to a beaker containing the load. This mixture was stirred for 15 min, and decanted into the column. In order to minimize the loading time, a bulb was used to exert pressure from the top of the column to increase the flow rate. After the loading was complete, the column was washed to baseline with 20 CV of equilibration buffer at a flow rate of 2 mL/min. Four fractions of 5 CV were collected for analytical purposes. The column was washed with 5 CV at a flow rate of 1 mL/min with a 50 mM imidazole buffer (100 mM potassium phosphate, pH 8.0, 500 mM NaCl, 5 mM 2-mercaptoethanol, 20% glycerol, 1.4 µg/mL leupeptin, 1.0 µg/mL pepstatin A and 50 mM imidazole). The protein was eluted with a 500 mM imidazole buffer (100 mM potassium phosphate, pH 8.0, 500 mM NaCl, 5 mM 2-mercaptoethanol, 20% glycerol, 1.4 µg/mL leupeptin, 1.0 µg/mL pepstatin A and 500 mM imidazole). The eluted fractions were pooled based on SDS-PAGE and protein concentration. The pooled protein was dialyzed against a 200 mM NaCl buffer (50 mM Hepes pH 7.5, 200 mM NaCl, 10 mM 2-

mercaptoethanol and 20% glycerol) overnight, using a dialysis tubing with a MWCO of 12-14 kDa(Spectrum Laboratories, Rancho Dominguez, CA).

The protein concentration and salt concentration were measured, and the sample was diluted to a final salt concentration of 100 mM using a buffer with no salt (50 mM Hepes, pH 7.5, 10 mM 2-mercaptoethanol and 20% glycerol). To concentrate the protein a sulfo-propyl (SP) column was packed (1 mL of resin per 40 mg of protein), and equilibrated with 10 CV with a 100 mM NaCl buffer (50 mM Hepes, pH 7.5, 10 mM 2-mercaptoethanol, 100 mM NaCl and 20% glycerol). The sample was loaded at a flow rate of 0.5 mL/min. The column was washed with 10 CV of 100 mM NaCl buffer. The protein was eluted with a 1 M NaCl buffer (50 mM Hepes, pH 7.5, 10 mM 2-mercaptoethanol, 1 M NaCl and 20% glycerol) in 1 CV fractions. The protein concentration was determined, and the sample dialyzed against a 300 mM NaCl buffer (50 mM Hepes, pH 7.5, 10 mM 2-mercaptoethanol, 300 mM NaCl and 20% glycerol) overnight. The protein concentration and the salt concentration were measured. The fractions were checked for RNAses and phosphatases. The protein was aliquoted, and stored at -80 ºC.

RNA Templates and Primers

Two RNA templates were obtained from Dharmacon for use in this study: a C-template with sequence 5'-AAAU**C**GAGAAGGAGAAAGCC-3' and a U-template with sequence 5'-AAAC**U**GAGAAGGAGAAAGCC-3'. The primers 5'-

GG-3' and 5'-pGG-3' were obtained from Dharmacon. pppGG was synthesized using standard laboratory procedures with PV RdRp.

Synthesis and Purification of pppGG using PV RdRp

A 1 mL reaction containing 10 µM $[ACC]_5$, 50 mM Hepes, pH 7.5, 10 mM 2-mercaptoethanol, 5 mM $MnCl_2$ and 1 mM GTP was initiated with 5 µM PV RdRp. The reaction was aliquoted into 8 tubes, and placed in a thermocycler (Progene) for 30 min at 30 ºC. The tubes were centrifuged, and the supernatant transferred to a 15 mL conical tube. The pooled sample was diluted with 0.4 M triethylammonium acetate (TEAA), pH 6.6 to a final concentration of 0.2 M. A Sep-Pak C18 filter column was washed with 10 mL acetonitrile, and equilibrated with 0.2 M TEAA, pH 6.6. The sample was passed three times through the filter, and the OD_{260} was measured. Then, the filter was washed with 3 mL 0.2 M TEAA, pH 6.6, and the sample was eluted with 3 mL acetonitrile into two 3 mL Falcon tubes. The sample was dried using a speed-vac, and suspended in 50 µL $T_{10}E_1$ (10 mM Tris, pH 8.0 and 1 mM EDTA, pH 8.0). A 25% acrylamide/3% bis-acrylamide denaturing gel was used to purify pppGG utilizing a vertical slab gel electrophoresis unit (Model SE 410, Hoefer) [23]. To isolate the RNA from the polyacrylamide gel, the gel was cut into small pieces, and placed inside of a 15 mL conical tube. Two milliliters of 0.2 M TEAA, pH 6.6 were added, and the sample incubated at 37 ºC for 40 min, shaking at 300 rpm. The supernatant was saved, and fresh 0.2 M TEAA, pH 6.6 was added. The above procedure was repeated a total of 5 times. The OD_{260} was measured for each fraction to make

sure the RNA was being isolated. All fractions were combined, and a new Sep-Pak C18 filter was washed and equilibrated as described above. The sample was passed three times through the filter, washed with two fractions of 1.5 mL 0.2 M TEAA, pH 6.6, followed by 1 mL of distilled water, and then the RNA eluted as described above. The sample was dried as described above, and suspended in 100 µL $T_{10}E_{0.1}$ (10 mM Tris, pH 8.0 and 0.1 mM EDTA, pH 8.0). The OD_{260} was measured and the extinction coefficient (DV NS5: 216,645 $M^{-1}cm^{-1}$, DV RdRp: 171,350 $M^{-1}cm^{-1}$ and HCV NS5B: 83, 770 $M^{-1}cm^{-1}$) used to determine the concentration.

Purification of RNA Oligos and Deprotection

PAGE was used to purify the RNA templates [26]. The RNA oligonucleotides were deprotected by removing the 2'-OH groups as follows: The oligonucleotide was suspended using 0.5 µL of 500 mM acetic acid per nmole of RNA, vortexed for 30 s and spun in a centrifuge. The mixture was incubated for 15 min at 65 °C, vortex for 30 s, and spun in a centrifuge. 0.5 µL of 660 mM Tris base per 1 nmole of RNA was then added, and the above procedure was repeated. A 1:10 dilution was used to measure the OD_{600} and the concentration calculated using the extinction coefficients.

Purity of [α-^{32}P] NTPs

[α-^{32}P] NTPs (MP Biomedicals LLC, Solon, OH) were diluted 1:100, and spotted in triplicate onto TLC plates. TLC plates were developed in 0.3 M

potassium phosphate, pH 7.0, dried and exposed to a phosphorimage screen. Imaging and quantitation were accomplished using ImageQuant 5.0 software (GE). The purity was used to correct the specific activity in the reactions.

Poly r (G) Polymerase Specific Activity Assay (*De Novo*)

Reactions contained 50 mM Hepes, pH 7.5, 5 mM $MgCl_2$, 10 mM 2-mercaptoethanol, 500 μM GTP, 0.2 μCi/μL [α-^{32}P] GTP, 100 μM poly (rC) and 1 μg enzyme. Components were incubated for 5 min at 30 °C before initiating the reaction with enzyme. Reactions were quenched to a final concentration of 50 mM EDTA. Products were analyzed by DE81 filter binding. Five μL of the quenched reactions were spotted in DE81 filter paper discs and dried. The discs were washed three times for 5 min with 5% dibasic sodium phosphate, and rinsed with 95% ethanol. Radioactivity was quantitated by liquid scintillation counting using 5 mL of Ecoscint scintillation fluid (National Diagnostics).

Primer Extension Assay

A reaction containing 50 mM HEPES, pH 7.5, 10 mM 2-mercaptoethanol, 5 mM $MgCl_2$, 10 μM CTP, 10 μM UTP, 0.07 μCi/μL [α-^{32}P] CTP, 2.5 μM of U-template and pppGG was initiated with enzyme. After 40 min, 25 μM heparin was added. The assembled DV NS5-15mer complex was used in rapid quench-flow experiments.

Rapid Chemical-Quench Flow Experiments

Rapid mixing/quenching experiments were performed using a chemical quench flow apparatus (model RQF-3, KinTek Corp., Snow Shoe, PA). Experiments were performed at 30 ºC using a circulating water bath. DV NS5 in complex with a 15mer RNA oligonucleotide in 50 mM HEPES, pH 7.5, 10 mM 2-mercaptoethanol, 5 mM $MgCl_2$, and 25 μM heparin was rapidly mixed with various ATP concentrations in 50 mM HEPES, pH 7.5, 10 mM 2-mercaptoethanol and 5 mM $MgCl_2$, and quenched by the addition of 0.3 M EDTA.

Product Analysis: Denaturing Polyacrylamide Gel Electrophoresis

For all bench top experiments, samples were quenched with loading buffer (90% formamide, 0.025% bromophenol blue, 0.025% xylene cyanol and 100 mM EDTA). Quenched samples from rapid quench-flow experiments were mixed with equal amounts of loading buffer. Five μL of samples heated to 65 ºC for 5 min were loaded onto a 20% or 25% denaturing polyacrylamide gel containing 1X TBE and 7 M urea. Gels were run at 85 watts, and visualized by phosphorimager. Quantitation was done with ImageQuant 5.0 software as described above. Data were fit by non-linear regression using the program KaleidaGraph (Synergy Software, Reading, PA). The data from the time courses of product formation were fit to a double-exponential equation:

Product = $(-A_1)\,(\exp(-k_{obs,1}t)) - (A_2)\,(\exp(-k_{obs,2}t)) + A_3$, where A_1 is the amplitude for the fast phase, $k_{obs,1}$ is the observed rate constant for the fast phase, A_2 is the

amplitude for the slow phase, $k_{obs,2}$ is the observed rate constant for the slow phase and A_3 is the amplitude for both phases. The apparent binding constant ($K_{d,app}$) and maximum rate constant for nucleotide incorporation (k_{pol}) were determined using the equation: $k_{obs} = (k_{pol}[NTP])/(K_{d,app} + [NTP])$.

Chapter 3

Results

Purification of DV NS5, DV RdRp and HCV NS5B

The protein was extracted from the cells, subjected to polyethylamine precipitation (PEI) to remove nucleic acids, and to ammonium sulfate precipitation serving as an early step for the removal of protein contaminants. A two-step purification was established (see Chapter 2). In the first step, the protein was bound to the nickel column and was then eluted with imidazole. In the second step, the protein was concentrated using a sulfopropyl (SP) column (Fig. 6A). All concentrated fractions were checked for contaminants, and no RNAses or phosphatases were detected (data not shown). The purity of all proteins was greater than 95% (Fig. 6B,C,D). The molecular weight of DV NS5, DV RdRp and HCV NS5B is 104 kDa, 74 kDa and 64 kDa, respectively.

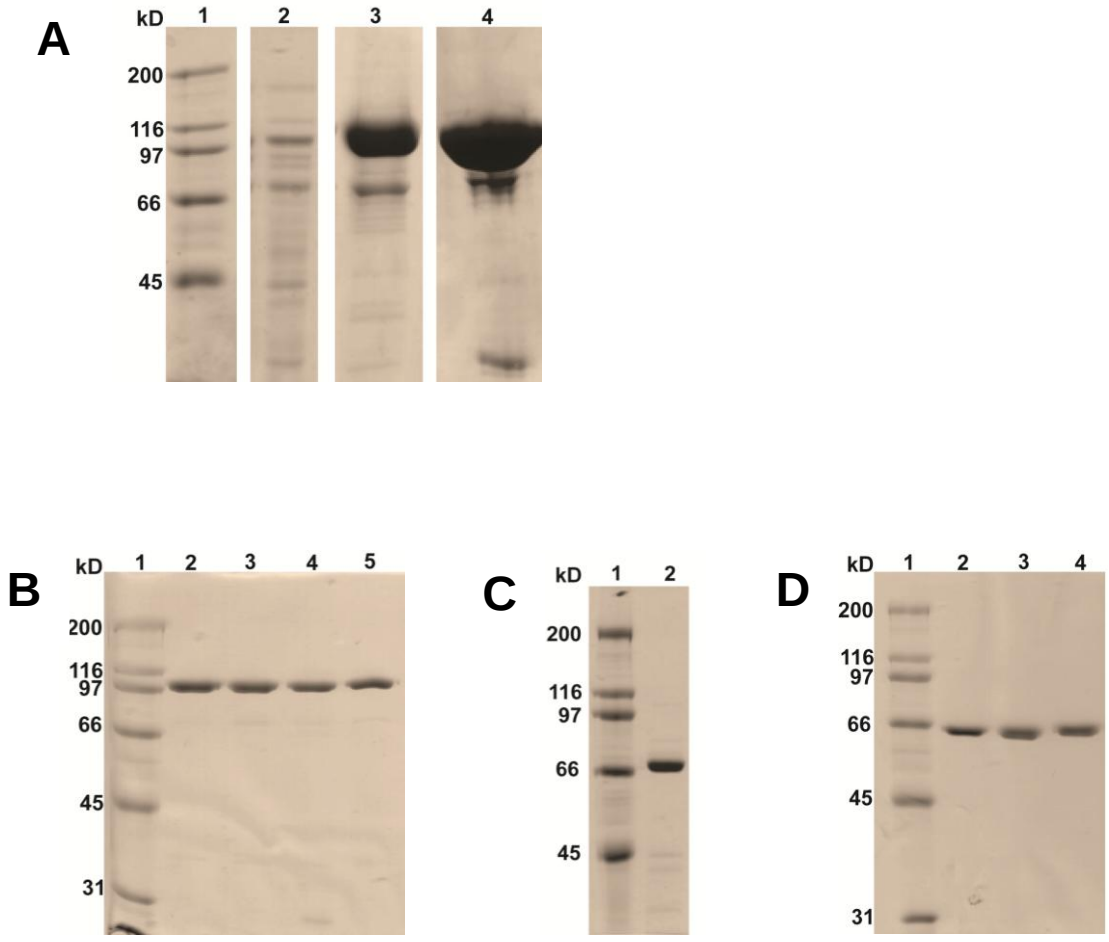

Figure 6: Purification of DV NS5, DV RdRp and HCV NS5B.
Representative CHis protein purification (DV NS5). (1) MW marker (2) Nickel column load (3) SP column load (4) Concentrated protein. (**B)** 1 µg DV NS5 proteins. (1) MW marker (2) K689 (3) K689R (4) K689H (5) K689Q. **(C)** 1 µg DV RdRp. (1) MW marker (2) DV RdRp. (**D)** 1 µg HCV NS5B proteins. (1) MW marker (2) K355 (3) K355R (4) K355Q.

The Methyltransferase Domain Contributes to the Polymerase Activity of DV NS5

The enzymatic activities of DV NS5 and DV RdRp were determined using a poly (rG) activity assay as described in Material and Methods. The specific activity (SA) was determined in the presence of Mg^{2+} from three experiments. For DV NS5, the SA was 95.9 ± 1.1 pmol GMP/min/μg enzyme. A deletion of the methyltransferase domain reduced the RdRp activity by 10-fold to a value of 9.9 ± 0.6 pmol GMP/min/μg enzyme (Fig.7A). Mn^{2+} was used to rule out that the reduced enzymatic activity was due to the protein being inactive. Studies performed by Selisko et al. suggested RdRp domain was fully active [27]. In the presence of Mn^{2+}, DV RdRp is 15-fold more active with an SA of 145.8 ± 6.1 pmol GMP/min/μg enzyme (Fig. 7B). In addition, an increased by 2-fold was observed for DV NS5 in the presence of Mn^{2+}, with a value of 211.8 ± 8.0 pmol GMP/min/μg enzyme. Either in Mn^{2+} or Mg^{2+}, the enzymatic activity of DV NS5 is higher than DV RdRp.

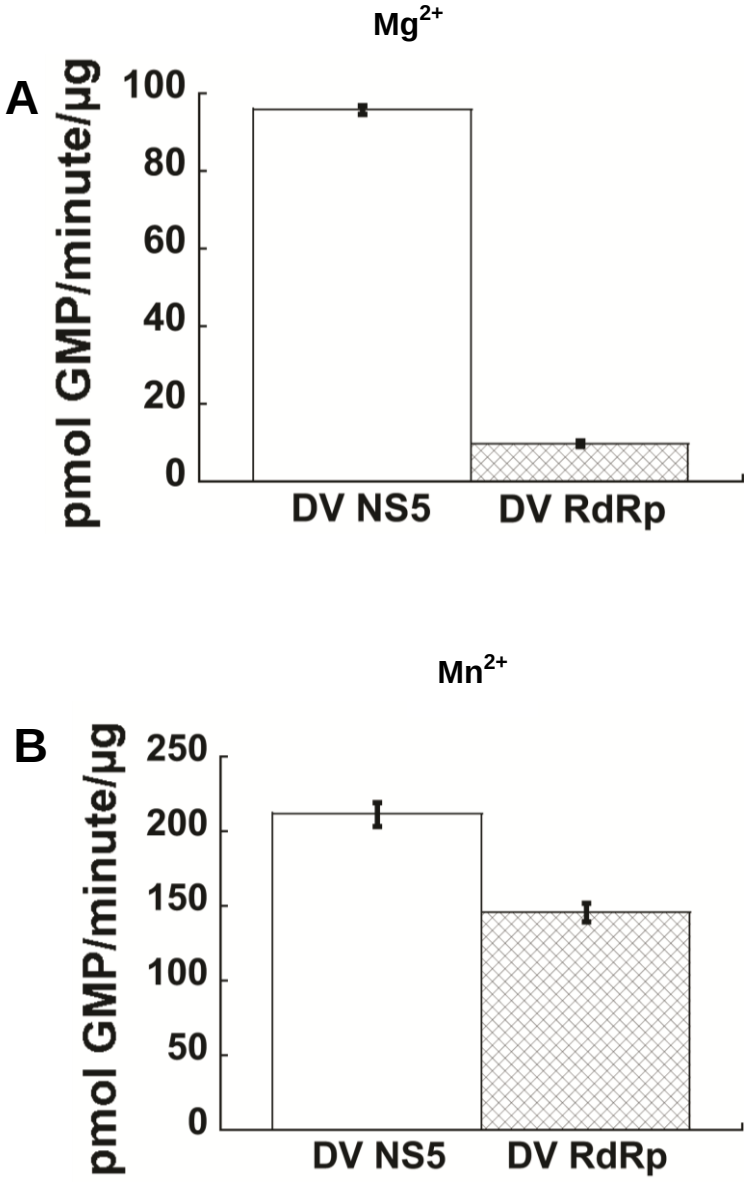

Figure 7: The Methyltransferase Domain Contributes to the Polymerase Activity of DV NS5. (**A)** The specific activity of DV NS5 and DV RdRp was measured in the presence of 5 mM Mg^{2+} at 5 min. DV NS5 specific activity was 95.9 ± 1.1 pmol GMP/min/µg enzyme and DV RdRp specific activity was 9.9 ± 0.6 pmol GMP/min/µg enzyme. **(B)** The specific activity of DV NS5 and DV RdRp was measured in the presence of 5 mM Mn^{2+} at 5 min. DV NS5 specific activity was 211.8 ± 8.0 pmol GMP/min/µg enzyme and DV RdRp specific activity was 145.8 ± 6.1 pmol GMP/min/µg enzyme.

DV NS5 has a Preference for 5' Phosphorylated Primers

Three dinucleotide primers were examined: lacking phosphate groups (GG), with one phosphate group (pGG) and triphosphorylated (pppGG). In addition, *de novo* initiation with a high concentration of GTP was tested. A difference in primer utilization by DV NS5 was observed throughout the time course (Fig. 8B,C). 3mer formation at 90 min with 10 μM GG, pGG or pppGG was 0.93, 4.36 and 7.79 μM, respectively. With 100 μM primer, the values were 5.19, 8.66, and 11.08 μM, respectively. The reaction with 500 μM GTP looking at *de novo* initiation was very inefficient, with only 0.62 μM of 3mer formed (data not shown).

Differential Mobility of Phosphorylated Trinucleotide Products

During electrophoresis of nucleic acids in denaturing polyacrylamide gels, products are resolved based on molecular weight, but we observed that the number of phosphate groups on trinucleotides affect mobility in a manner distinct from molecular weight alone. In a 25% denaturing polyacrylamide gel, pGGC and pppGGC mobility was the same, and GGC ran slower (Fig. 8D). However, on a 20% gel, a difference between pGGC and pppGGC mobility was observed, but the distance between pppGGC and GGC did not correlate with the absence of three phosphates (Fig. 8E). In order to confirm the identity of the products observed, pppGGC was treated with shrimp alkaline phosphatase (SAP). A reaction with GGC and pppGGC served as control. Early in the time course,

laddering of pppGGC into ppGGC, pGGC and GGC was observed, confirming that the phosphate groups of short products influence the mobility (Fig. 8F).

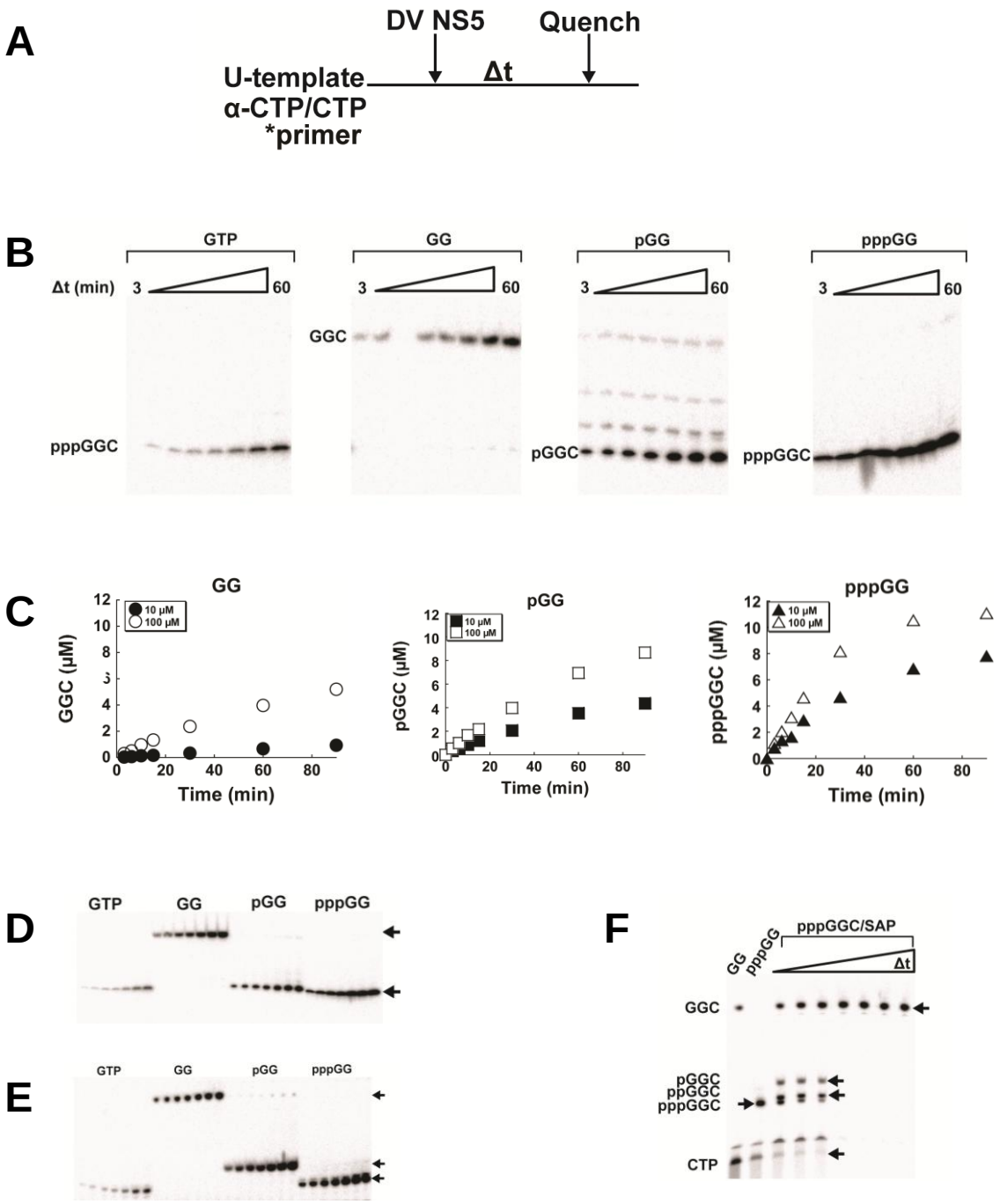

Figure 8: DV NS5 has a Preference for 5' Phosphorylated Dinucleotides. **(A)** Experimental design. The reaction was initiated with enzyme, and quenched at the indicated times. (**B)** Samples were run on a 25% denaturing polyacrylamide gel (10 μM primer experiment shown). **(C)** Kinetics of 3mer formation with 10 μM and 100 μM primers. **(D)** 20% denaturing polyacrylamide gel. pGGC and pppGGC mobility is the same **(E)** 25% denaturing polyacrylamide gel. pGGC and pppGGC migration is different. **(F)** Time course of pppGGC treated with shrimp alkaline phosphatase (SAP).

The Preference for Phosphorylated Primers is not Observed in HCV NS5B

The presence of 5'-phosphates on primers did not influence their utilization by HCV NS5B (Fig. 9). At 90 min, with 10 μM GG, 7.75 μM of 3mer was formed (Fig 9C). With pGG and pppGG the values were 11.14 and 5.20 μM (Fig 9C), respectively. As with DV NS5, the *de novo* reaction yielded the lowest amount of 3mer, with 2.8 μM (data not shown).

DV NS5 Does not Initiate RNA Synthesis with GDP

It was previously reported that HCV NS5B utilizes GDP as an initiator nucleotide [18]. In a reaction with DV NS5 with 1 mM GDP, and increasing concentrations of GTP, no additional bands were observed on the gel other than the pppGGC product, suggesting that DV NS5 has a specific requirement for the first nucleotide to be triphosphorylated (Fig. 10A). On the other hand, in a reaction with HCV NS5B and 1 mM GDP, titration of GTP led to formation of ppGGC (Fig. 10B).

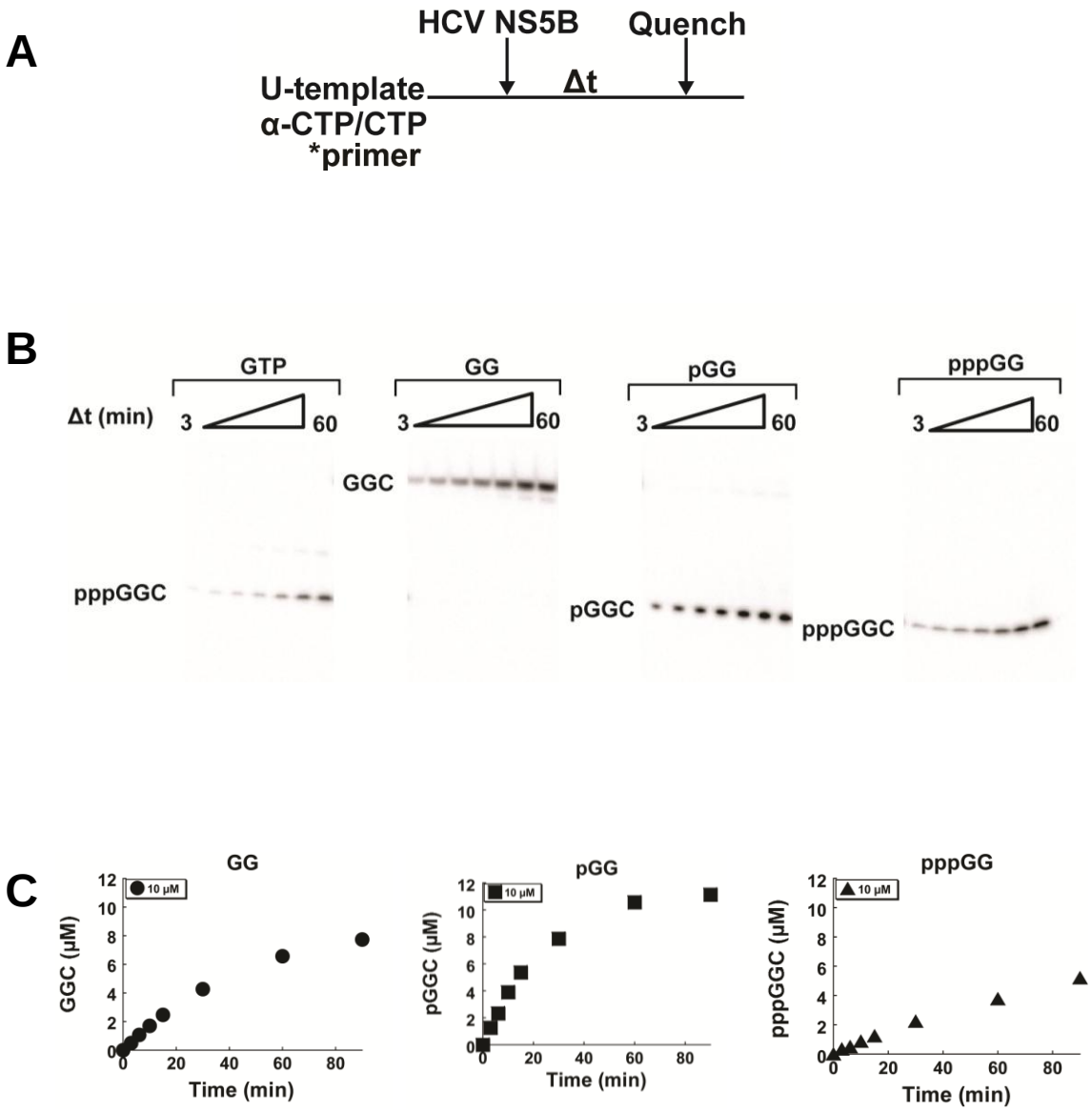

Figure 9: For HCV NS5B the Presence of 5' Phosphates on Dinucleotide Primers did not Correlate with 3mer Formation. (**A)** Experimental design. The reaction was initiated with enzyme, and quenched at the indicated times. **(B)** Samples were run on a 25% denaturing polyacrylamide gel. (**C)** Kinetics of 3mer formation with 10 μM GG, 10 μM pGG or 10 μM pppGG.

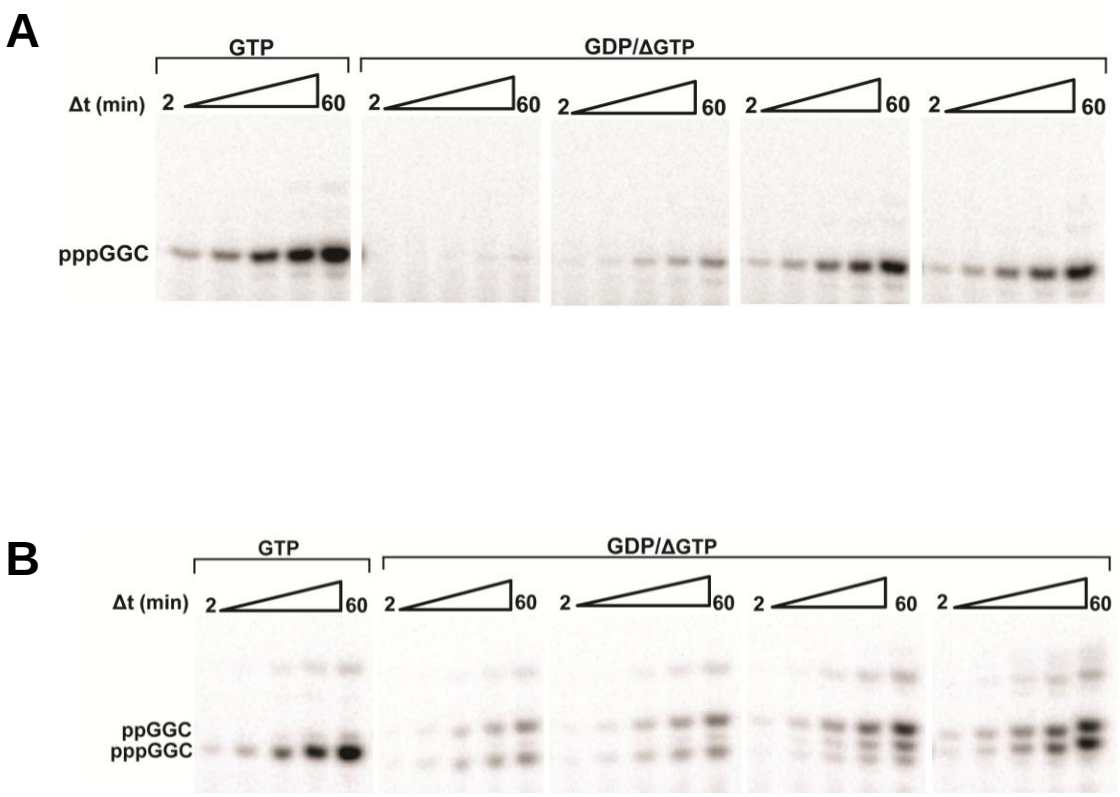

Figure 10: DV NS5 Does not Initiate RNA Synthesis with GDP. (A) DV NS5. GTP was titrated in the presence of GDP. The formation of ppGGC was not osbserved. (**B)** HCV NS5B. GTP was titrated in the presence of GDP, and the formation of ppGGC was observed with increasing GTP concentrations.

DV NS5 Motif-D Lysine is Required for High Nucleotidyl Transfer Efficiency

Four different derivatives of DV NS5 were purified, having Lys (WT), Arg, His or Gln at the general acid position (Fig. 6B). Enzymatic activity was determined using a poly (rG) activity assay. Interestingly, the nature of the amino acid correlated with the enzymatic activity. The SA for K689 was 95.9 ± 1.1 pmol GMP/min/μg enzyme, for K689R was 70.8 ± 1.6 pmol GMP/min/μg enzyme, for K689H was 1.3 ± 0.8 pmol GMP/min/μg enzyme and for K689Q was 0.6 ± 0.2 pmol GMP/min/μg enzyme (Fig. 11A).

On the other hand, HCV NS5B derivatives with Lys (WT), Arg or Gln at general acid position 355 did not reveal a difference in the enzymatic activity. The SA for K355 was 20.0 ± 2.2 pmol GMP/min/μg enzyme, for K355R was 24.7 ± 1.6 pmol GMP/min/μg enzyme and for K355Q was 26.4 ± 0.8 pmol GMP/min/μg enzyme (Fig. 11B).

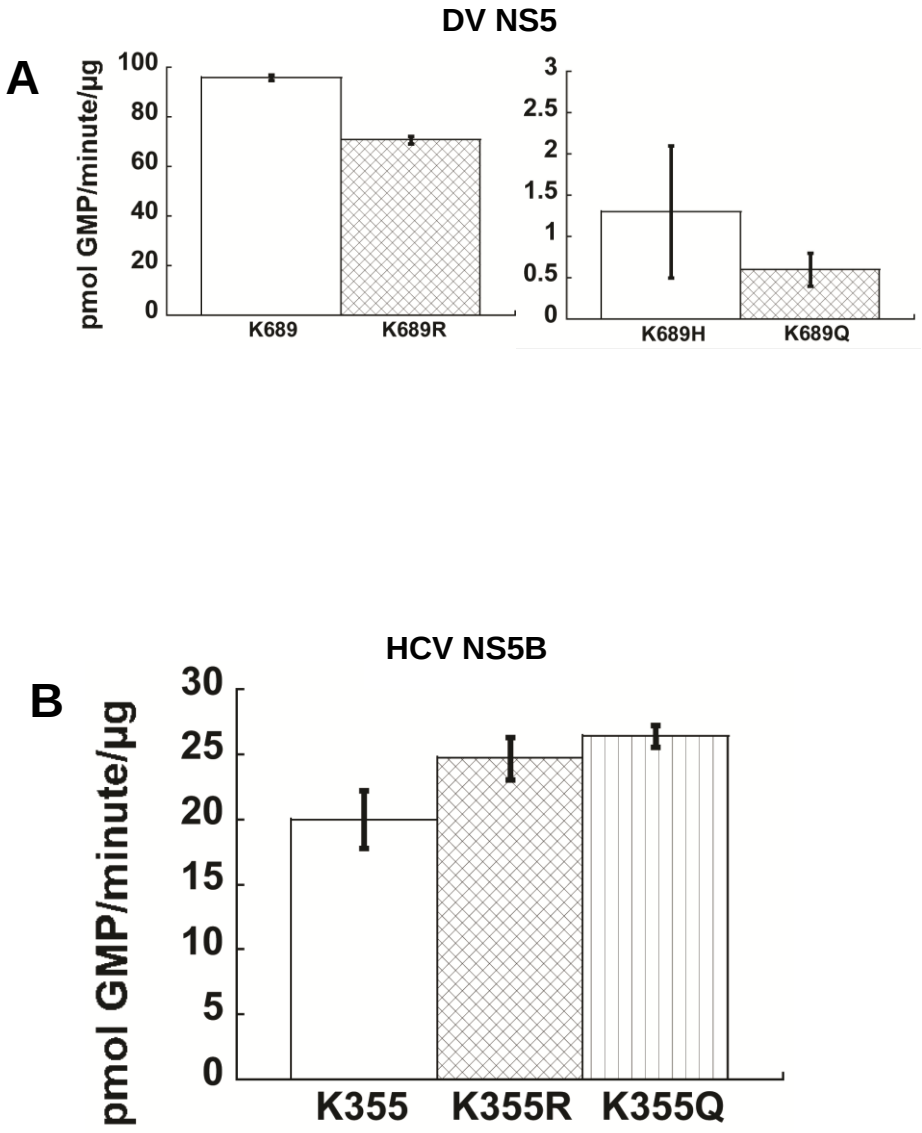

Figure 11: Specific Activity of DV NS5 and HCV NS5B General Acid Derivatives. (A) The specific activity for DV NS5 K689, K689R K689H and K689Q was 95.9 ± 1.1, 70.8 ± 1.6, 1.3 ± 0.8 and 0.6 ± 0.2 pmol GMP/min/µg enzyme, respectively. (**B)** The specific activity for HCV NS5B K355, K355R and K355Q was 20.0 ± 2.2, 24.7 ± 1.6 and 26.4 ± 0.8 pmol GMP/min/µg enzyme, respectively.

DV NS5 General Acid Derivatives: Initiation versus Elongation with pppGG

To further confirm a defect in DV NS5 general acid derivatives for nucleotidyl transfer, experiments were accomplished to examine at the initiation and elongation phase using the primer pppGG. During initiation, the kinetics of trinucleotide formation by K689, K689R and K689H were similar, and for K689Q was slower (Fig. 12A,B,C). In contrast, during the elongation phase all derivatives exhibited a defect in the amount of product accumulated in comparison to the wild-type enzyme. (Fig. 12D,E,F)

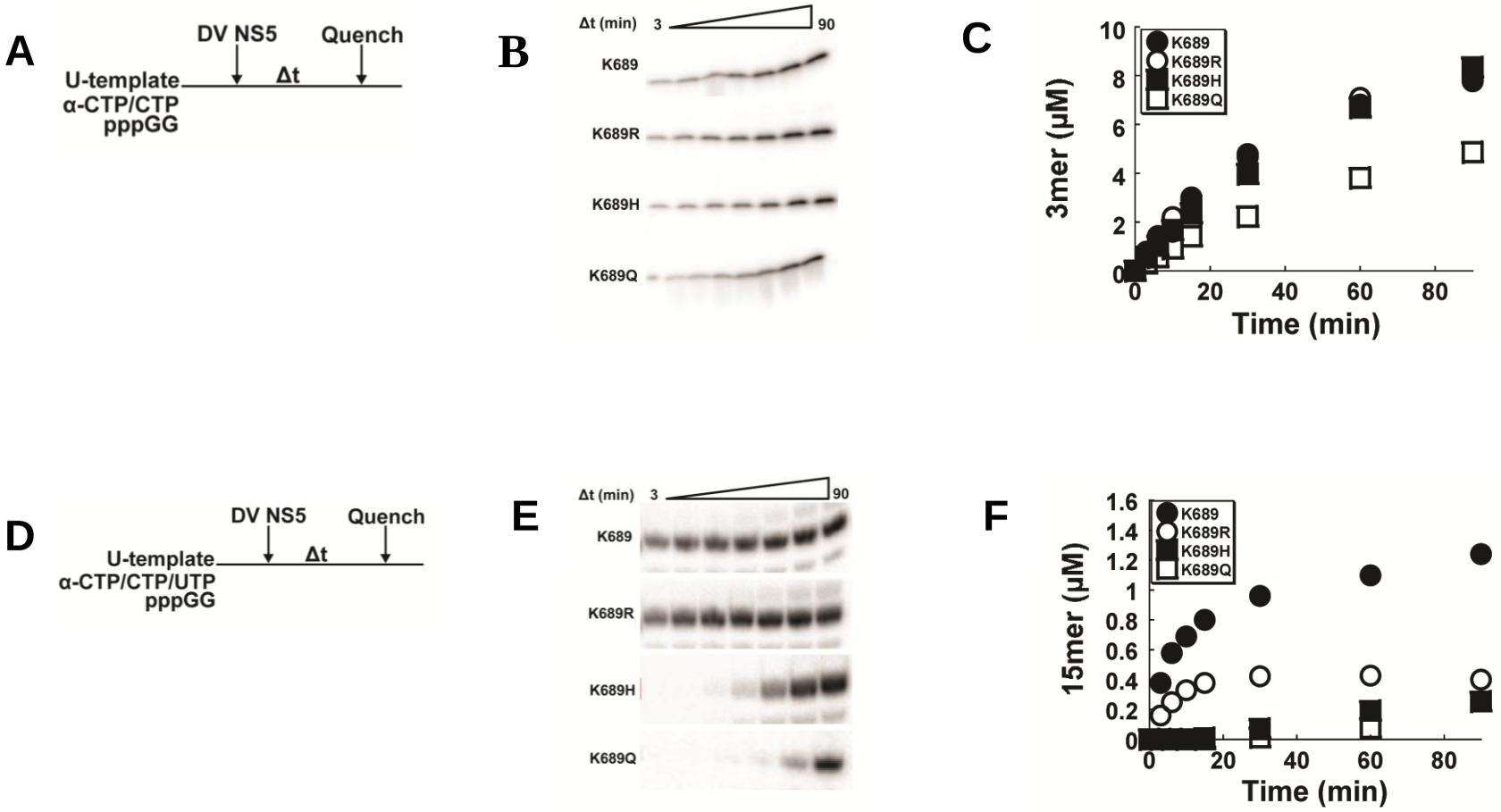

Figure 12: DV NS5 General Acid Derivatives Exhibited a Defect During the Elongation Phase, but not During the Initiation Phase. (A) Experimental design (3mer formation). A reaction containing CTP was initiated with enzyme, and quenched at the indicated times. **(B)** Samples were resolved in a 25% denaturing polyacrylamide gel. **(C)** Kinetics of 3mer formation for K689, K689R, K689H and K689Q. **(D)** Experimental design (15mer formation). A reaction with CTP and UTP was initiated with enzyme, and quenched at the indicated times. **(E)** Samples were resolved in a 25% denaturing polyacrylamide gel. **(F)** Kinetics of 15mer formation for K689, K689R, K689H and K689Q.

Optimal [NaCl] and [Heparin] to Study DV NS5 Elongation Complexes

In order to establish optimal assay conditions to study DV NS5 single nucleotide incorporation during the elongation phase, NaCl was titrated. As the NaCl concentration increased, the concentration of assembled complex decreased (Fig. 13A). Based on this assay, a salt concentration less or equal to 50 mM is optimal for complex assembly. Heparin was used to trap the polymerase that is not in complex with the RNA. The optimal concentration of heparin required to trap 1 μM of DV NS5 was 25 μM (Fig. 13B).

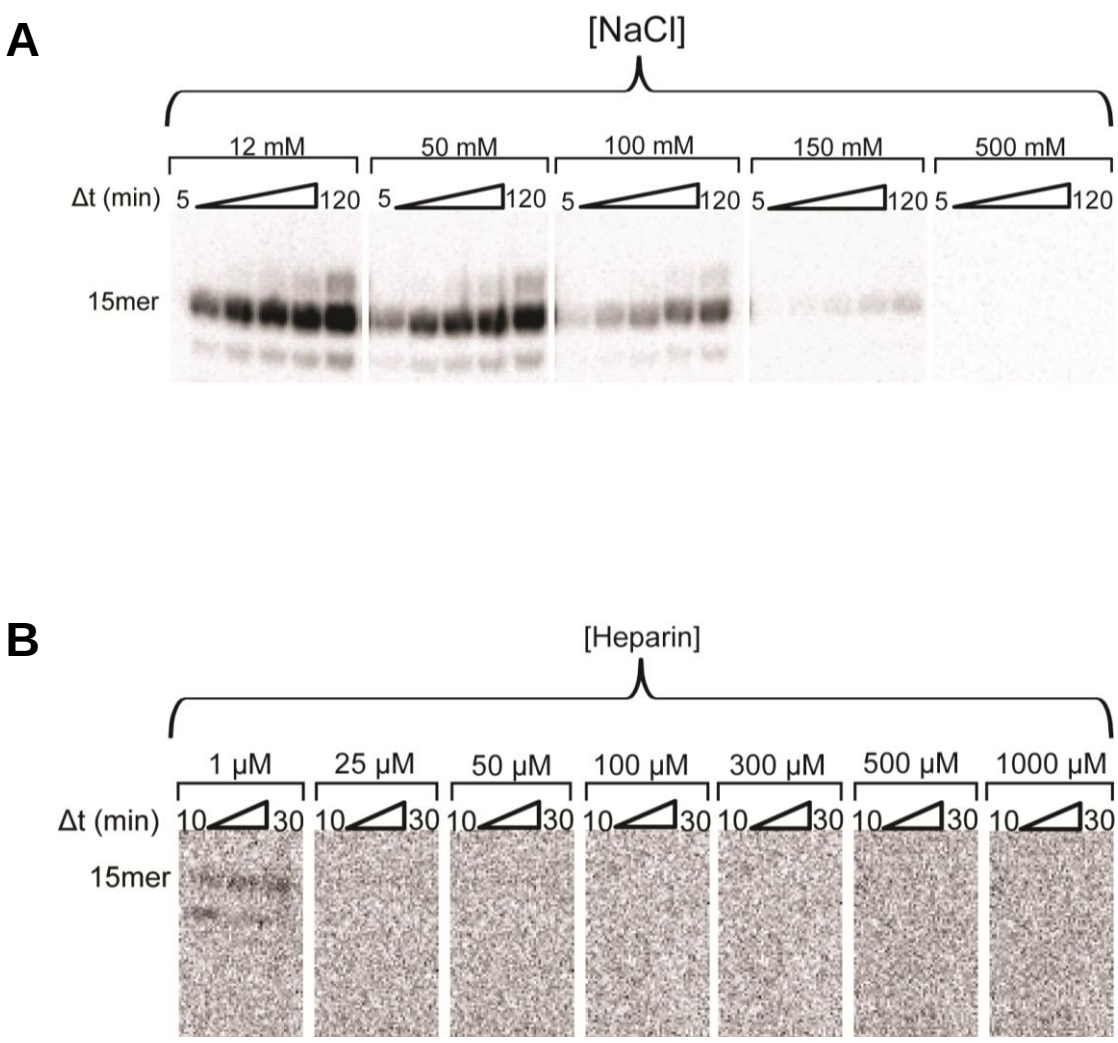

Figure 13: Optimal [NaCl] and [Heparin] to Study DV NS5 Elongation Complexes. (A) Assembly of DV NS5 is affected by the NaCl concentration. (**B)** Titration of heparin to determine the concentration required to trap 1 μM DV NS5.

DV NS5 Assembles in Stable Complexes Competent for AMP Incorporation

To assess the stability of DV NS5 elongation complexes, assembly was permitted to occur for 40 min, heparin trap was added, and at various time points thereafter, elongation was initiated by addition of ATP. Reactions were quenched with 50 mM EDTA 30 s after ATP addition. Only a 12% reduction in complex concentration, as reported by 16mer product formation, was observed 90 min after addition of heparin. In the pre-steady state experiments, the maximum time the complex is sitting after the addition of heparin is less than 30 min, with only a 5% loss of active complex over time (Fig. 14B,C). This experiment confirms adequate complex stability to examine pre-steady state elongation phase AMP incorporation in the chemical quench-flow instrument.

Pre-steady-state Kinetics of DV NS5

The kinetics of single correct nucleotide incorporation from DV NS5 assembled complex were studied at various NTP concentrations to determine the maximum rate constant for nucleotide incorporation (k_{pol}) and the apparent dissociation constant ($K_{d,app}$) for nucleotide substrate. Assembled complexes were rapidly mixed with 50, 100, 250, 500 or 1000 μM ATP in the chemical quench-flow instrument. The time courses for product formation at various ATP concentrations, shown in Fig. 15B, were best fit to a double-exponential equation (Fig. 15B). Rate constants for the fast phase and slow phase were plotted as a function of ATP concentration, and the data were fit to a hyperbola. For the fast

phase, the $K_{d,app}$ was 203 ± 54 μM and the k_{pol} was 163 ± 15 s^{-1} (Fig. 15C). For the slow phase, the $K_{d,app}$ was 89 ± 19 μM and the k_{pol} was 15 ± 1 s^{-1} (Fig. 15D).

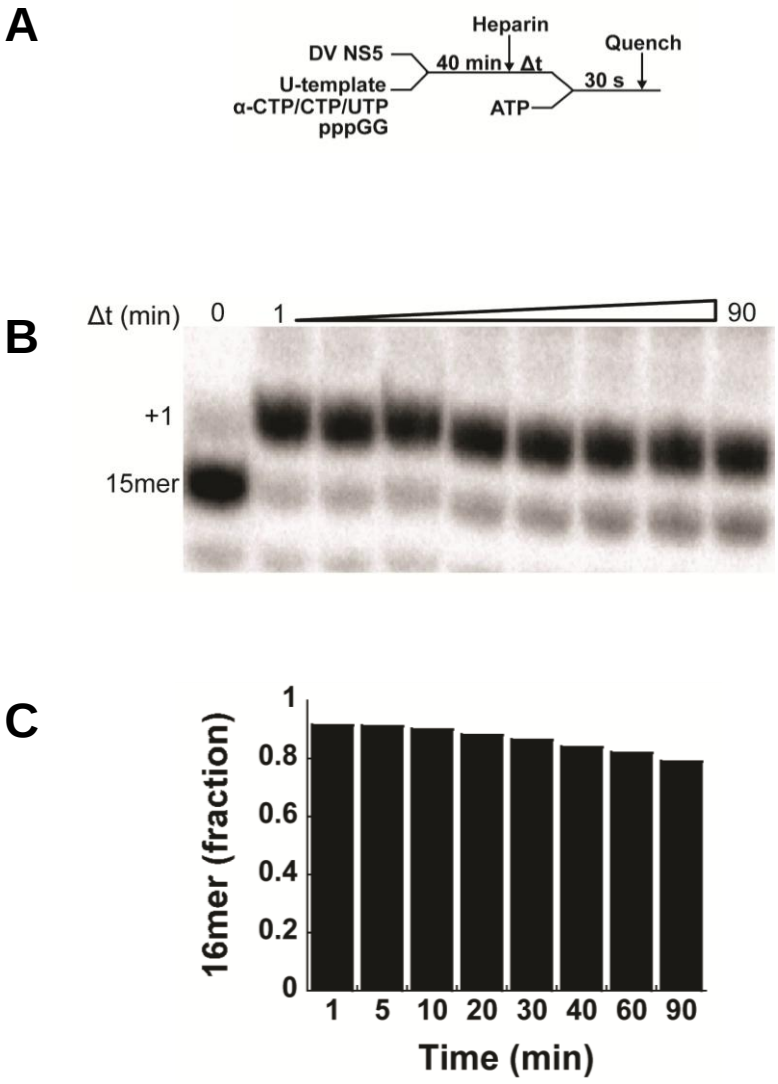

Figure 14: DV NS5 Assembles in Stable Complexes Competent for AMP Incorporation (A) Experimental design. After the addition of heparin, the reaction was mixed with ATP at the indicated times, and after 30 s quenched. **(B)** Samples were resolved in a 20% denaturing polyacrylamide gel. **(C)** Shown is the time course of 16-mer product formation from the experiment described in A.

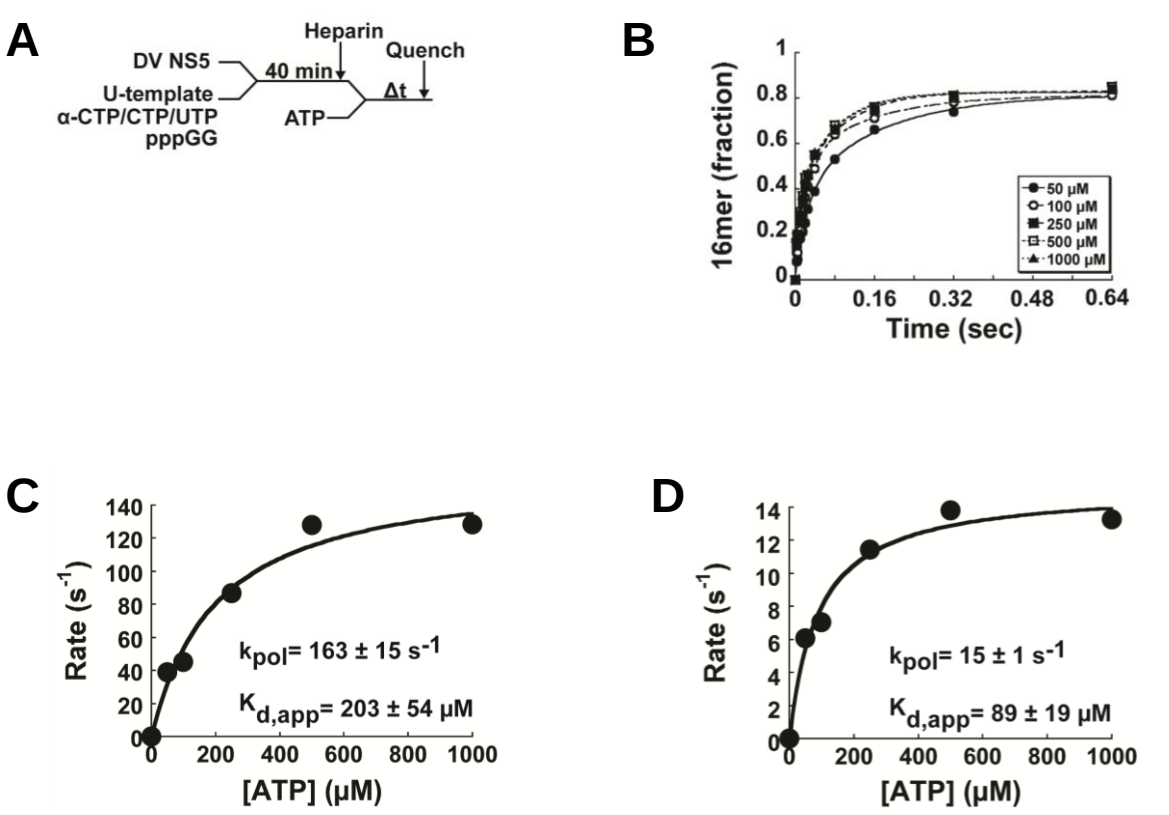

Figure 15: Pre-steady-state Kinetics of DV NS5 Elongation Phase Incorporation of AMP. (A) Experimental design. After the addition of heparin, the reaction was rapidly mixed with ATP in a chemical quench-flow instrument at the indicated times. **(B)** Kinetics of 16mer formation at 50, 100, 250, 500 and 1000 μM ATP. The data were fit to a double-exponential equation. **(C)** The observed rate constants of the fast phase were plotted as a function of ATP concentration, and fit to a hyperbola, yielding a $K_{d,app}$ of 203 ± 54 μM and k_{pol} of 163 ± 15 s^{-1}. **(D)** The observed rate constants of the slow phase were plotted as a function of ATP concentration and fit to a hyperbola, yielding a $K_{d,app}$ of 89 ± 19 μM and k_{pol} of 15 ± 1 s^{-1}.

Chapter 4

Discussion

The Methyltransferase Domain is Required for RdRp Activity

Viral RNA polymerases use different strategies to initiate the replication of their genome. They have evolved to either initiate *de novo* or in a primer-dependent manner (Fig. 5)[16]. The *Flaviviridae* family of viruses initiates *de novo*, but differ in the strategy used for the translation of the RNA by ribosomes. They can use an internal ribosomal entry site or a capped RNA for translation [28-30].

Examples of viruses that cap their genome are Yellow Fever virus, West Nile virus and Dengue virus. The required enzyme activities to cap the RNA are supplied by NS3 and NS5. NS3 has the RNA 5'-triphosphatase (RTPase) activity [31, 32], and NS5 has the guanylyltransferase (GTase), the N7-methyltransferase (N7-MTase) and the 2'O-MTase activity [10, 33-35]. In combination, they produce $^{7Me}GpppN_{2'OMe}$ at the 5' end of the viral genome. In addition to the methyltransferase activity, NS5 also possesses the RdRp activity required to replicate the genome [9, 36].

In these studies, Mg^{2+} was utilized as the divalent cation allowing us to make a direct comparison between DV NS5 and DV RdRp. The deletion of the methyltransferase domain directly impacted the nucleotide incorporation activity of DV NS5. Others have suggested the methyltransferase domain is not required for RdRp activity [27]**.** DV NS5 specific activity was 95.9 ± 1.1 pmol GMP/min/µg

enzyme. On the other hand, DV RdRp showed a 10-fold decrease in specific activity, with a value of 9.9 ± 0.6 pmol GMP/min/μg enzyme. Although crystal structures for the methyltransferase domain and the RdRp domain are available, attempts to crystallize the complete DV NS5 protein consisting of both domains have been unsuccessful. Our data suggest that the methyltransferase domain plays a critical role in the catalytic activity of the RdRp domain. The domains are linked by an interdomain region. It is not known how these two domains interact, but protein-protein interactions might be necessary to maintain the structural and functional integrity of the RdRp domain. Currently, it is not understood how RNA synthesis and capping are coordinated. It would also be interesting to determine how the interaction of DV NS5 and NS3 modulate RNA synthesis, and if this complex is able to cap short RNA products.

Yap et al. reported that the DV RdRp domain possesses less activity than full length NS5, but their assays were carried out with a combination of Mn^{2+} and Mg^{2+} [9]. Mn^{2+} has been shown to decrease the specificity for nucleotide incorporation by polymerases, causing uncertainty about interpretation of data [37, 38]. They developed a high throughput screen (HTS) to test inhibitory compounds. However, correlation between *in vitro* and *in vivo* studies is complicated by the use of Mn^{2+}, since it is not the biologically relevant divalent cation [39]. In the presence of Mn^{2+}, we observed a 15-fold increase in enzymatic activity compared to the reaction with Mg^{2+} for DV RdRp, ruling out that the protein was inactive (Fig. 7B). Although, DV RdRp enzymatic activity increases in Mn^{2+}, the enzymatic activity of DV NS5 in Mn^{2+} is still higher (Fig. 7B).

DV NS5 has a Preference for Triphosphorylated Dinucleotides

Replication of a viral RNA by a polymerase that initiates *de novo* consists of three phases: initiation, initiation to elongation transition, and elongation. The accumulation of short abortive products has been observed *in vitro* for eukaryotic and prokaryotic RNA polymerases [25, 40, 41]. Recently, accumulation of abortive products was observed *in vivo* in *E. coli* [25]. Accumulation of short RNA products might be a requirement for the transition between initiation and elongation, and perhaps DV NS5 utilizes these products to efficiently elongate RNA.

Using three different dinucleotide primers (GG, pGG and pppGG) we observed a preference by DV NS5 for the triphosphorylated form. In a reaction examining at 3mer formation, the order of efficiency of primer utilization was pppGG>pGG>GG (Fig. 8). On the other hand, with HCV NS5B, a correlation could not be established between the presence of phosphates at the dinucleotide primer 5'-end and efficiency of primer utilization. The order of efficiency of utilization was pGG>GG>pppGG (Fig. 9). In addition, we confirmed that HCV NS5B can use GDP as the initiating nucleotide, as previously reported [21], but DV NS5 has a strict requirement for the first nucleotide to be triphosphorylated (Fig. 10).

The preference for the phosphorylated form of the primer by DV NS5 presumably reflects the fact that viral polymerases that cap their genome must have a triphosphorylated 5'-end to initiate the capping reaction. This implies a

need to have higher affinity toward substrates that are triphosphorylated. In contrast, HCV NS5B did not show the same correlation as DV NS5. This might be expected, as the translation of the HCV genome is not affected by the presence of phosphates at the 5'-end. In addition, *de novo* initiation was examined in the presence of high concentration of GTP, and found that 3mer accumulation was lower than when primers were used. A possible reason is that the accumulation of short abortive products might be a requirement for an efficient transition between the initiation and elongation phase, as others have suggested [41].

DV NS5 Motif-D Lysine is Required for Efficient Nucleotidyl Transfer

The motif-D general acid residue is involved in protonation of the pyrophosphate leaving group during the nucleotidyl transfer reaction. In PV RdRp, a change at the general acid position from Lys to Arg reduced the rate constant for nucleotide incorporation and increased fidelity [15] (Smidansky, Maksimchuk and Cameron unpublished). Moreover, an engineered poliovirus with Arg at the general acid position protected mice against a challenge with wild-type virus, demonstrating potential for the development of an engineered virus for vaccine purposes (Lee, August and Cameron unpublished).

In DV NS5, the general acid Lys is located at position 689, and this residue is conserved across all Dengue serotypes. Using a poly r (G) assay, we determined the SA of DV NS5 K689, K689R, K689H and K689Q. Interestingly, the highest enzymatic activity was observed for K689 followed by K689R, K689H

and K689Q, respectively. This is consistent with findings for PV RdRp general acid derivatives (data not shown). On the other hand, for HCV NS5B a decreased in the specific activity was not observed between K355, K355R and K355Q. In addition, the specific activity of HCV NS5B was about 4-fold lower in comparison to DV NS5. Altogether, this data suggests HCV NS5B does not use the general acid for nucleotidyl transfer.

To further characterize the DV NS5 general acid derivatives, we looked at the initiation phase (3mer formation) and the elongation phase (15mer formation), utilizing pppGG as primer. A defect in initiation was not observed for DV NS5 K689, K689R or K689H (Fig. 12A,B,C). On the other hand, a defect in elongation (15mer formation) was observed for DV NS5 K689R, K689H and K689Q in comparison to DV NS5 K689 WT (Fig 12D,E,F).

The kinetic scheme for transcription initiation and elongation by T7 RNAP reveals a rate-limiting step after binding of polymerase to promoter DNA and before the transition from initiation to elongation [42]. An explanation for why DV NS5 K689, K689R and K689H produced the same amount of 3mer may be that the rate limiting step is binding to the RNA. Thus, the defect in nucleotide incorporation is masked. During elongation, a defect is observed for all DV NS5 general acid derivatives suggesting Dengue virus utilizes the general acid for nucleotidyl transfer.

Kinetics of Single Nucleotide Incorporation During the Elongation Phase

A detailed study of the kinetics of single nucleotide incorporation during the elongation phase for DV NS5 has been lacking. Structurally, DV NS5 possesses a priming loop that protrudes into the active site, preventing binding of dsRNA (Fig. 2A) In other systems, the ability of polymerases to bind double-stranded substrates has facilitated kinetic analysis [43, 44].

This is the first study reporting the characterization of nucleotide incorporation during the elongation phase for the full length DV NS5. The NaCl concentration used for complex formation was 12 mM (Fig 13A). Higher salt concentrations had an inhibitory effect on complex assembly. The concentration of heparin used was 25 μM. At this concentration, the formation of 15mer was inhibited, indicating that all enzyme was trapped (Fig. 13B).

The ability of DV NS5-RNA complex to incorporate a single nucleotide after the addition of ATP was then examined. A loss of 12% active complex was observed 90 min after assembly. In pre-steady state experiments, the last time point was taken by 30 min, so a loss of only 5% active complex was expected (Fig. 14).

The $K_{d,app}$ and k_{pol} values were determined using a chemical quench-flow instrument (Fig. 15B). The rate constant for the fast phase of the reaction represents the DV NS5-RNA productive complex. The rate constant for the slow phase likely represents the shift from a non-productive conformation to a productive conformation of the DV NS5-RNA complex. A $K_{d,app}$ of 203 ± 54 μM

and a k_{pol} of 163 ± 15 s^{-1} was observed for the fast phase (Fig. 15C), and a $K_{d,app}$ of 89 ± 19 μM and a k_{pol} of 15 ± 1 s^{-1} for the slow phase (Fig. 15D).

Jin et al. reported a $K_{d,app}$ of 275 ± 25 μM and a k_{pol} of 18± 1 s^{-1} for the fast phase of DV RdRp in complex with a double-stranded substrate for GMP incorporation [45]. For the fast phase, our $K_{d,app}$ value is similar, but the k_{pol} was 9 fold higher for AMP incorporation. The difference in the rate constant for nucleotide incorporation between DV RdRp and DV NS5 might be explained by the substrate utilized. The double stranded substrate used in their study has a blunt end, only allowing nucleotide incorporation in one direction. It might be possible that most of the enzyme was bound in the wrong orientation, and the fraction available to elongate was not in a productive complex conformation. Evidence that might support this is the fact that in their active site titration, only 15% of the DV RdRp was active.

Chapter 5

Conclusion and Future Direction

An assay to study the kinetics of single nucleotide incorporation by DV NS5 was developed. Since Mg^{2+} is used as the source of divalent cation, this assay has the potential for testing the potency and efficacy of future nucleoside analogues. Moreover, using this assay it might be possible to study the interaction between DV NS3 and DV NS5, and perhaps reconstitute the capping machinery *in vitro*. With no evidence on how replication and RNA capping is coordinated, it would be interesting to examine if capped dinucleotides are used as primers more efficiently than pppGG. It has been suggested that as the newly synthesized RNA is exiting through the RdRp tunnel, capping happens after presumably [46]. If this holds true, then capping of the RNA might not occur independently from replication, and possibly this could be tested *in vitro*.

The role of the methyltransferase domain for optimal RdRp activity has been demonstrated. Whether the defect observed is during binding to RNA or nucleotide addition it is yet to be determined. This evidence suggests that the most biologically relevant form of the enzyme for biochemical analysis is DV NS5. Another important finding was the preference for triphosphorylated primers by DV NS5. This observation may mean that viruses which initiate *de novo* and utilize their own capping mechanism might have evolved to recognize primers that are triphosphorylated.

Finally, utilizing DV NS5 general acid derivatives, it was confirmed that the use of the general acid catalyst occurs within the *Flaviviridae* family. As demonstrated with poliovirus, the development of an attenuated Dengue virus vaccine based on a single amino acid change might be possible.

The absence of an effect for HCV NS5B merits further study. This difference may underlie mechanisms required for the establishment of a persistent infection.

References

1. Chambers, T.J., et al., *Flavivirus genome organization, expression, and replication.* Annu Rev Microbiol, 1990. 44: p. 649-88.
2. Moradpour, D., F. Penin, and C.M. Rice, *Replication of hepatitis C virus.* Nat Rev Microbiol, 2007. 5(6): p. 453-63.
3. Suzuki, T., et al., *Molecular biology of hepatitis C virus.* J Gastroenterol, 2007. 42(6): p. 411-23.
4. Tellinghuisen, T.L., et al., *Studying hepatitis C virus: making the best of a bad virus.* J Virol, 2007. 81(17): p. 8853-67.
5. Poordad, F., et al., *Boceprevir for Untreated Chronic HCV Genotype 1 Infection.* New England Journal of Medicine, 2011. 364(13): p. 1195-1206.
6. Kyle, J.L. and E. Harris, *Global spread and persistence of dengue.* Annu Rev Microbiol, 2008. 62: p. 71-92.
7. Gubler, D.J., *Dengue and dengue hemorrhagic fever.* Clinical Microbiology Reviews, 1998. 11(3): p. 480-+.
8. King, N.J.C., et al., *Immunopathology of flavivirus infections.* Immunology and Cell Biology, 2007. 85(1): p. 33-42.
9. Yap, T.L., et al., *Crystal structure of the dengue virus RNA-dependent RNA polymerase catalytic domain at 1.85-Angstrom resolution.* Journal of Virology, 2007. 81(9): p. 4753-4765.
10. Zhou, Y.S., et al., *Structure and function of flavivirus NS5 methyltransferase.* Journal of Virology, 2007. 81(8): p. 3891-3903.
11. Dong, H.P., B. Zhang, and P.Y. Shi, *Flavivirus methyltransferase: A novel antiviral target.* Antiviral Research, 2008. 80(1): p. 1-10.
12. Steitz, T.A., *A mechanism for all polymerases.* Nature, 1998. 391(6664): p. 231-2.
13. Steitz, T.A. and J.A. Steitz, *A General 2-Metal-Ion Mechanism for Catalytic Rna.* Proceedings of the National Academy of Sciences of the United States of America, 1993. 90(14): p. 6498-6502.
14. Yang, W., J.Y. Lee, and M. Nowotny, *Making and breaking nucleic acids: two-Mg2+-ion catalysis and substrate specificity.* Mol Cell, 2006. 22(1): p. 5-13.
15. Castro, C., et al., *Nucleic acid polymerases use a general acid for nucleotidyl transfer.* Nature Structural & Molecular Biology, 2009. 16(2): p. 212-218.
16. van Dijk, A.A., E.V. Makeyev, and D.H. Bamford, *Initiation of viral RNA-dependent RNA polymerization.* J Gen Virol, 2004. 85(Pt 5): p. 1077-93.
17. Choi, K.H., et al., *The structure of the RNA-dependent RNA polymerase from bovine viral diarrhea virus establishes the role of GTP in de novo initiation.* Proc Natl Acad Sci U S A, 2004. 101(13): p. 4425-30.
18. Ferrer-Orta, C., et al., *A comparison of viral RNA-dependent RNA polymerases.* Curr Opin Struct Biol, 2006. 16(1): p. 27-34.
19. Kao, C.C., P. Singh, and D.J. Ecker, *De novo initiation of viral RNA-dependent RNA synthesis.* Virology, 2001. 287(2): p. 251-60.
20. Kim, M.J., et al., *Template nucleotide moieties required for de novo initiation of RNA synthesis by a recombinant viral RNA-dependent RNA polymerase.* J Virol, 2000. 74(22): p. 10312-22.

21. Ranjith-Kumar, C.T., et al., *Requirements for de novo initiation of RNA synthesis by recombinant flaviviral RNA-dependent RNA polymerases.* J Virol, 2002. 76(24): p. 12526-36.
22. Ranjith-Kumar, C.T., et al., *De novo initiation pocket mutations have multiple effects on hepatitis C virus RNA-dependent RNA polymerase activities.* J Virol, 2004. 78(22): p. 12207-17.
23. Nomaguchi, M., et al., *De novo synthesis of negative-strand RNA by Dengue virus RNA-dependent RNA polymerase in vitro: nucleotide, primer, and template parameters.* J Virol, 2003. 77(16): p. 8831-42.
24. Luo, G., et al., *De novo initiation of RNA synthesis by the RNA-dependent RNA polymerase (NS5B) of hepatitis C virus.* J Virol, 2000. 74(2): p. 851-63.
25. Goldman, S.R., R.H. Ebright, and B.E. Nickels, *Direct Detection of Abortive RNA Transcripts in Vivo.* Science, 2009. 324(5929): p. 927-928.
26. Arnold, J.J. and C.E. Cameron, *Poliovirus RNA-dependent RNA polymerase (3D(pol)). Assembly of stable, elongation-competent complexes by using a symmetrical primer-template substrate (sym/sub).* J Biol Chem, 2000. 275(8): p. 5329-36.
27. Selisko, B., et al., *Comparative mechanistic studies of de novo RNA synthesis by flavivirus RNA-dependent RNA polymerases.* Virology, 2006. 351(1): p. 145-158.
28. Lewis, J.D. and E. Izaurralde, *The role of the cap structure in RNA processing and nuclear export.* European Journal of Biochemistry, 1997. 247(2): p. 461-469.
29. Kieft, J.S., *Viral IRES RNA structures and ribosome interactions.* Trends Biochem Sci, 2008. 33(6): p. 274-83.
30. Fraser, C.S. and J.A. Doudna, *Structural and mechanistic insights into hepatitis C viral translation initiation.* Nature Reviews Microbiology, 2007. 5(1): p. 29-38.
31. Benarroch, D., et al., *The RNA helicase, nucleotide 5'-triphosphatase, and RNA 5'-triphosphatase activities of Dengue virus protein NS3 are Mg2+-dependent and require a functional Walker B motif in the helicase catalytic core.* Virology, 2004. 328(2): p. 208-18.
32. Xu, T., et al., *Structure of the Dengue virus helicase/nucleoside triphosphatase catalytic domain at a resolution of 2.4 A.* J Virol, 2005. 79(16): p. 10278-88.
33. Issur, M., et al., *The flavivirus NS5 protein is a true RNA guanylyltransferase that catalyzes a two-step reaction to form the RNA cap structure.* RNA, 2009. 15(12): p. 2340-50.
34. Egloff, M.P., et al., *Structural and functional analysis of methylation and 5 '-RNA sequence requirements of short capped RNAs by the methyltransferase domain of dengue virus NS5.* Journal of Molecular Biology, 2007. 372(3): p. 723-736.
35. Egloff, M.P., et al., *An RNA cap (nucleoside-2 '-O-)-methyltransferase in the flavivirus RNA polymerase NS5: crystal structure and functional characterization.* Embo Journal, 2002. 21(11): p. 2757-2768.
36. Ackermann, M. and R. Padmanabhan, *De novo synthesis of RNA by the dengue virus RNA-dependent RNA polymerase exhibits temperature dependence at the initiation but not elongation phase.* Journal of Biological Chemistry, 2001. 276(43): p. 39926-39937.
37. Tabor, S. and C.C. Richardson, *Effect of manganese ions on the incorporation of dideoxynucleotides by bacteriophage T7 DNA polymerase and Escherichia coli DNA polymerase I.* Proc Natl Acad Sci U S A, 1989. 86(11): p. 4076-80.

38. **Huang, Y., et al.,** ***Determinants of ribose specificity in RNA polymerization: effects of Mn2+ and deoxynucleoside monophosphate incorporation into transcripts.*** **Biochemistry, 1997. 36(44): p. 13718-28.**
39. **Zhang, R.Q. and K.J. Ellis,** ***Invivo Measurement of Total-Body Magnesium and Manganese in Rats.*** **American Journal of Physiology, 1989. 257(5): p. R1136-R1140.**
40. **Martin, C.T., D.K. Muller, and J.E. Coleman,** ***Processivity in Early Stages of Transcription by T7-Rna Polymerase.*** **Biochemistry, 1988. 27(11): p. 3966-3974.**
41. **Moroney, S.E. and J.A. Piccirilli,** ***Abortive Products as Initiating Nucleotides during Transcription by T7 Rna-Polymerase.*** **Biochemistry, 1991. 30(42): p. 10343-10349.**
42. **Skinner, G.M., et al.,** ***Promoter binding, initiation, and elongation by bacteriophage T7 RNA polymerase. A single-molecule view of the transcription cycle.*** **J Biol Chem, 2004. 279(5): p. 3239-44.**
43. **Werneburg, B.G., et al.,** ***DNA polymerase beta: Pre-steady-state kinetic analysis and roles of arginine-283 in catalysis and fidelity.*** **Biochemistry, 1996. 35(22): p. 7041-7050.**
44. **Arnold, J.J. and C.E. Cameron,** ***Poliovirus RNA-dependent RNA polymerase (3Dpol): pre-steady-state kinetic analysis of ribonucleotide incorporation in the presence of Mg2+.*** **Biochemistry, 2004. 43(18): p. 5126-37.**
45. **Jin, Z.N., et al.,** ***Characterization of the Elongation Complex of Dengue Virus RNA Polymerase ASSEMBLY, KINETICS OF NUCLEOTIDE INCORPORATION, AND FIDELITY.*** **Journal of Biological Chemistry, 2011. 286(3): p. 2067-2077.**
46. **Malet, H., et al.,** ***Crystal structure of the RNA polymerase domain of the West Nile Virus non-structural protein 5.*** **Journal of Biological Chemistry, 2007. 282(14): p. 10678-10689.**